peroxides were quantified in terms of TBARS according to the method of Nagano *et al.* (24). Lipoproteins (20 μg of protein) were suspended in 0.2 ml of 150 mM NaCl. The suspension was mixed with 0.5 ml of 20% (w/v) trichloroacetic acid and 0.5 ml of the reagent (335 mg of 2-thiobarbituric acid in 100 ml of 50% (v/v) acetic acid). The mixture was boiled at 95 °C for 60 min. After being cooled, 2.0 ml of 1-butanol was added, shaken vigorously, and centrifuged at 4000 × *g* for 10 min. The fluorescence of supernatant was measured with excitation at 515 nm and emission at 550 nm. Tetramethoxypropane was used as a standard. The electrophoretic mobility of native or oxidized LDL was measured in barbital/sodium barbital, pH 8.0, on 1% agarose gel SPE (Beckman Coulter, Fullerton, CA) (25). The lipoprotein pattern was visualized by staining the film with a lipid-specific stain. Relative electrophoretic mobility was defined as ratio of the distances migrated from the origin by modified LDL *versus* native LDL. For analysis of the degradation of apoB, lipoproteins were delipidated with ethyl acetate: ethanol (1:1), solubilized with 10% SDS, and separated on 4% to 20% SDS gels (Invitrogen Japan K.K. Minato-ku, Tokyo, Japan.) at 30 mA for 1 h. After electrophoresis, samples were transferred onto nitrocellulose membranes (Bio-Rad) by using semi-dry blotting, and the membranes were incubated with polyclonal rabbit antibody to apoB at a dilution of 1:1000 for 2 h. After washing, the membranes were stained with horseradish peroxidase-conjugated goat anti-rabbit antibody (Santa Cruz Biotechnology). Antigen detection was performed with an ECL plus kit (GE Healthcare UK Ltd., Buckinghamshire, England). Immunoreactive bands were quantified by using National Institutes of Health Image analysis software (26), and the data represent the percentage of intact apoB in modified LDL *versus* native LDL.

Full-length PPARs System—The reporter plasmid $(AOX)^3$-luc, containing tree copies of an upstream activating sequence for the PPAR response element of acyl-CoA oxidase and a thymidine kinase gene promoter (tk-promoter) in front of a luciferase cDNA, and PPARγ2 expression plasmid (pCMX-PPARγ2), containing the mouse PPARγ2 gene driven by the CMV promoter, were kindly gifted from Dr. Michael Brownlee (Dept. of Medicine, Diabetes Research Center, Albert Einstein College of Medicine, Bronx, NY). Human PPARα expression plasmid (pCMV-hPPARα) containing the human PPARα gene driven by the CMV promoter was a kind gift from Dr. Takahide Miyamoto and Dr. Tomoko Kakizawa (Dept. of Aging Medicine and Geriatrics, Shinshu University School of Medicine, Japan) (27). To measure the PPARα or PPARγ activity, RAW264.7 cells (2×10^6 cells/well) were transfected with $(AOX)^3$-luc, and pCMV-hPPARα or pCMX-PPARγ2 using Lipofectamine 2000 (Invitrogen). Cells were also co-transfected with a *Renilla* luciferase plasmid (pRL-SV40, Promega, Madison, WI) as an internal control. Luciferase assay was performed as described below.

GAL4 Chimera System—The fusion protein expression vectors pM-PPARα and pM-PPARγ, containing residues 1–147 of the GAL4 DNA-binding domain and 167–467 of the human PPARα ligand-binding domain or 204–505 of the human PPARγ ligand-binding domain, driven by the SV40 promoter were described previously (28). The reporter plasmid p4xUASg-tk-luc, containing four copies of a 17-mer upstream activating sequence for the GAL4 DNA-binding domain and a thymidine kinase gene promoter (tk-promoter) in front of a luciferase cDNA, was also described previously (28). To measure the PPARα or PPARγ ligand binding activity, RAW264.7 cells (2×10^6 cells/well) were transfected with p4xUASg-tk-luc and pM-PPARα or pM-PPARγ, and subjected to luciferase assays as described below.

Luciferase Assays—The NF-κB luciferase reporter plasmid (pNF-κB-Luc) used for measuring NF-κB activity was purchased from Takara Bio, Inc. (Shiga, Japan). Luciferase reporter plasmids were transfected into RAW264.7cells, mouse peritoneal macrophages, or THP-1 macrophages (2×10^6 cells/well) using Lipofectamine 2000. Cells were also co-transfected with a *Renilla* luciferase plasmid (pRL-SV40, Promega) as an internal control. After transfection, the cells were cultured for 5 h, and compounds were added to the medium at appropriate concentrations. After an additional 24 h of incubation, the cells were lysed and subjected to luciferase assays using a Dual-Luciferase Reporter Gene Assay system (Promega) according to the manufacturer's instructions (29).

Transcription Activity of PPARs—Transcription activity of PPARα and PPARγ was assayed using an enzyme-linked immunosorbent assay-based PPARα, -δ, and -γ Complete Transcription Factor Assay Kit (Cayman Chemical). Sample proteins were extracted from aortas of $apoE^{-/-}$ or WT mice according to the manufacturer's instructions and were added to a 96-well plate that had been immobilized by an oligonucleotide containing PPAR response element. After 1 h, the wells were incubated with diluted primary PPARα or PPARγ antibody to recognize the accessible epitope on PPARα or PPARγ protein upon DNA binding. The horseradish peroxidase-conjugated secondary antibody was added, and incubation was conducted for 1 h. At the end, the reaction was stopped, and absorbance was read at 450 nm on a spectrophotometer. This assay is specific for PPARα or PPARγ activation, and there is no cross-reaction with other PPAR isoforms.

Transfection of siRNA—The siRNA against COX-2, PPARα, PPARγ, and an irrelevant 21-nucleotide siRNA duplex as a control were purchased from Santa Cruz Biotechnology. RAW264.7 cells (2×10^6 cells/well) or mouse peritoneal macrophages (2×10^6 cells/well) were transfected with the siRNA of COX-2, PPARα, PPARγ, or control, in the absence or presence of appropriate plasmids using Lipofectamine 2000 (Invitrogen). After 4-h incubation, the medium was changed to medium A, and luciferase assay or real-time RT-PCR was performed. In comparison to the control siRNA, the siRNA of COX-2, PPARα, or PPARγ suppressed the expression of these proteins by 86, 72, or 77%, respectively, according to Western blot analysis (11).

Adenoviral Vectors—Cells were infected with a recombinant replication-deficient adenovirus containing each of the following genes: dominant negative ERK (DN-ERK) and p38 MAPK (DN-p38 MAPK) for 48 h at the multiplicity of infection of ~50, as described previously (26, 30), and were allowed to recover in medium A for 3 h. This condition conferred expression of LacZ as a marker gene in nearly 100% of transfected cells (26, 30).

Western Blot Analysis—Cells (2×10^6 cells/well in 6-well plate, Nunc) or aortic sinus tissues were lysed by the lysis buffer, and centrifuged ($20,000 \times g$ at 4 °C for 10 min). Supernatants were used as sample proteins. Protein concentrations were determined by the Micro BCA Protein Assay Reagent (Pierce), according to the protocol recommended by the manufacturer. Samples were applied to 10% SDS gels and transferred to nitrocellulose membranes (Bio-Rad) by using semi-dry blotting. Membranes were incubated with the indicated antibodies at a dilution of 1:1000 for 2 h. After washing, the membranes were stained with horseradish peroxidase-conjugated goat anti-rabbit or anti-mouse antibodies (Santa Cruz Biotechnology). Antigen detection was performed with ECL plus kit (GE Healthcare UK Ltd.). Immunoreactive bands were quantified by using NIH Image (26).

Real-time RT-PCR Analysis—Macrophages (2×10^6 cells/well) were incubated with or without the indicated effectors. Total RNA was extracted with TRIzol (Invitrogen). The first strand cDNA synthesis containing 1 μg of total RNA was primed with oligo(dT). To quantify gene transcripts, the Light-Cycler System (Roche Molecular Biochemicals, Indianapolis, IN) was used (29). PCRs were performed using SYBR Green I master mix and specific primers for mouse COX-2, ABCA1, MCP-1, and β-actin, which were designed as follows: COX-2, forward primer, 5′-CCAGAGCAGAGAGATGAAA-3′ and reverse primer, 5′-GGTACAGTTCCATGACATC-3′; ABCA1, forward primer, 5′-ATTGCCAGACGGAGCCG-3′ and reverse primer, 5′-TGCCAAAGGGTGGCACA-3′; MCP-1, forward primer, 5′-GGTCCCTGTCATGCTTCT-3′ and reverse primer, 5′-CATCTTGCTGGTGAATGAGT-3′; and β-actin, forward primer, 5′-AACACCCCAGCCATGTACG-3′ and reverse primer, 5′-ATACCCAAGAAGGAAGGCTG-3′. The quantitative results for COX-2, ABCA1, and MCP-1 were normalized by the levels of β-actin mRNA (11). To assess the specificity of the amplified PCR products, after the last cycle, a melting curve analysis was performed.

EIA for 15d-PGJ$_2$, PGE$_2$, and PGD$_2$—The 96-well-based EIA kit of 15d-PGJ$_2$, prostaglandin E$_2$ (PGE$_2$) or prostaglandin D$_2$ (PGD$_2$) was purchased from Cayman Chemical (Ann Arbor, MI). Cells cultured in 6-well plates or aortic sinus tissues were treated with the indicated effectors for 24 h, and then the cells were lysed with lysis buffer. To measure the amounts of 15d-PGJ$_2$ in lipoproteins, 40 μg of LDL or Ox-LDL were also suspended with the same lysis buffer. The concentrations of intracellular 15d-PGJ$_2$, PGE$_2$, and PGD$_2$ in cells or in lipoproteins were determined by each EIA kit according to the manufacturer's instructions (11).

Gas Chromatography—Gas chromatography of long chain fatty acids was performed commercially by SRL (Tokyo, Japan) (11). Briefly, cells (2×10^6 cells/well in 6-well plates) were incubated with the indicated effectors. After 24-h incubation, cells were counted using a Beckman Coulter Counter Z2. An aliquot (4×10^5 cells) of each sample was re-suspended in a glass tube, and the total lipids were extracted using Folch buffer (31). After hydrolysis with KOH, methyl esters of the fatty acids were prepared using BF_3 methanol. C23:0 was used as an internal standard. The esters were analyzed by gas chromatography using a Shimadzu GC-17A gas chromatograph equipped with a hydrogen flame ionization detector.

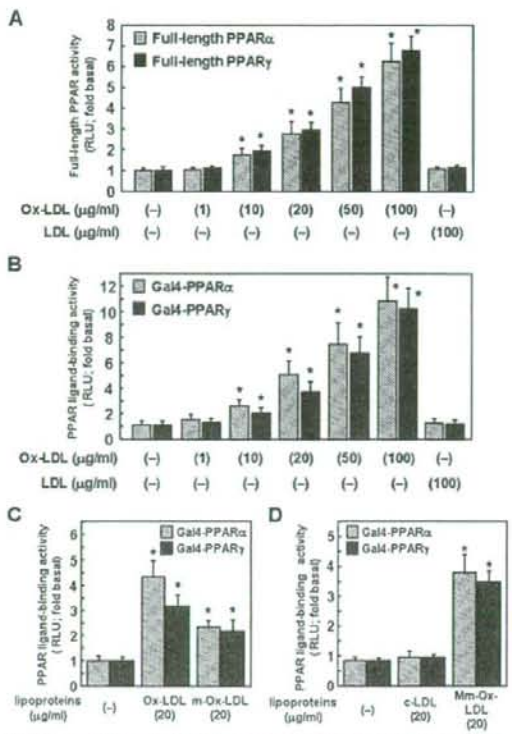

FIGURE 1. **Ox-LDL increases PPARα and PPARγ activities.** RAW264.7 cells were incubated with the indicated concentrations of native LDL, oxidized LDL (*Ox-LDL*), mildly oxidized LDL (*m-Ox-LDL*), control LDL (*c-LDL*), or macrophage-mediated Ox-LDL (*Mm-Ox-LDL*) for 24 h. PPARα or PPARγ activity was determined using the full-length PPARs system (*A*), and PPARα or PPARγ ligand binding activity was determined using the GAL4 chimera system (*B–D*). Data represent the mean ± S.E. of four separate experiments. *, $p < 0.01$ *versus* the controls.

Statistical Analysis—All data were expressed as the mean ± S.E. Differences between groups were examined for statistical significance by one-factor analysis of variance. $p < 0.05$ was considered to indicate a statistically significant difference.

RESULTS

Ox-LDL Induces PPARα and PPARγ Activation in Macrophages—We first examined the effect of Ox-LDL, which was prepared with 5 μM $CuSO_4$ for 20 h, on PPARα and PPARγ activation in RAW264.7 cells by full-length PPARα and PPARγ systems. As shown in Fig. 1*A*, Ox-LDL increased luciferase activity of both full-length PPARα and full-length PPARγ in a dose-dependent manner, whereas LDL had no effect.

We next examined the effect of Ox-LDL on PPARα and PPARγ ligand binding activity by the GAL4 chimera system. Ox-LDL also increased luciferase activity of both GAL4-PPARα and GAL4-PPARγ in a dose-dependent manner, whereas LDL had no effect (Fig. 1*B*). In similar experiments

TABLE 1

Modification of native LDL with $CuSO_4$ for 5 or 20 h

Native LDL was incubated with 5 μM $CuSO_4$ for 5 h (m-Ox-LDL) or for 20 h (Ox-LDL) at 37 °C, followed by the addition of 1 mM EDTA, and cooling. The modification of LDL was evaluated by TBARS, electrophoretic mobility, and degradation of apoB. Data represent the mean ± S.E. of four separate experiments.

	TBARS	Electrophoretic mobility (relative to LDL)	Intact apoB
	nmol MDA/mg LDL		*% of LDL*
LDL	2.2 ± 0.2	1	100
m-Ox-LDL	8.3 ± 0.5*	1.5 ± 0.1*	67.5 ± 2.2*
Ox-LDL	22.8 ± 1.2*	2.8 ± 0.2*	43.5 ± 1.8*

*$p < 0.01$ *versus* native LDL.

using mouse peritoneal macrophages and THP-1 macrophages, 50 μg/ml Ox-LDL increased PPARα ligand binding activity by 6.3- and 5.2-fold, and PPARγ ligand binding activity by 5.8- and 4.9-fold, respectively ($p < 0.01$, compared with control, data not shown).

Next, we prepared m-Ox-LDL, which was incubated with 5 μM $CuSO_4$ for 5 h, and investigated the effect of m-Ox-LDL on PPARα and PPARγ activation. As shown in Table 1, the modification of m-Ox-LDL estimated by TBARS, electrophoretic mobility, and apoprotein B degradation was lower than that of Ox-LDL incubated with 5 μM $CuSO_4$ for 20 h. Although the effects were slightly milder than that of Ox-LDL incubated for 20 h, m-Ox-LDL also significantly increased PPARα and PPARγ ligand binding activity (Fig. 1*C*).

To confirm the effect of cell-mediated oxidized LDL on PPARα and PPARγ activation, we prepared Mm-Ox-LDL. The oxidation of Mm-Ox-LDL, which was estimated by TBARS, was 7.1 ± 0.3 nmol of MDA/mg of LDL. On the other hand, we also prepared control LDL (c-LDL) by incubation with the same condition medium without macrophages. The TBARS of c-LDL was 2.4 ± 0.4 nmol of MDA/mg of LDL. As shown in Fig. 1*D*, Mm-Ox-LDL increased luciferase activities of both GAL4-PPARα and GAL4-PPARγ, whereas c-LDL had no effect.

COX-2 Is Involved in Ox-LDL-induced PPAR Activation—We next examined whether Ox-LDL induced COX-2 expression by real-time RT-PCR and Western blot analysis. After treatment of RAW264.7 cells with 40 μg/ml Ox-LDL, both COX-2 mRNA and protein were increased at 1 h, and these increases remained for up to 6 h (Fig. 2, *A* and *B*).

We then examined the effect of COX-2 inhibitors NS-398 and meloxicam on Ox-LDL-induced PPAR activation. Ox-LDL-induced activation of PPARα and PPARγ was partially but significantly inhibited by NS-398 and meloxicam (Fig. 2*C*). We further investigated the effect of COX-2 siRNA on Ox-LDL-induced PPARα and PPARγ activation. Treatment with siRNA for COX-2 down-regulated COX-2 protein expression by 86% (Fig. 2*D*) and inhibited Ox-LDL-induced PPARα and PPARγ activation by 58.8% and 56.1%, respectively (Fig. 2*E*).

Ox-LDL-induced COX-2 Expression Was Mediated by ERK1/2 Signals—We have previously reported that Ox-LDL can activate ERK1/2 and p38 MAPK (32), which are known to be involved in COX-2 expression induced by several stimuli in macrophages. Therefore, we speculated on the involvement of MAPK signals in Ox-LDL-induced COX-2 expression in macrophages. First, we performed time-course experiments of

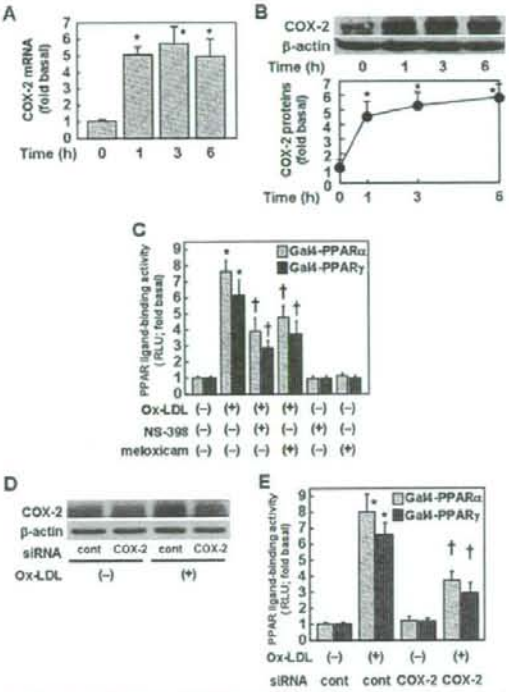

FIGURE 2. **Ox-LDL-induced COX-2 expression is involved in PPARα and PPARγ activation.** *A* and *B*, RAW264.7 cells were incubated with 40 μg/ml Ox-LDL for the indicated times. *A*, after incubation, total RNA was extracted, and the expression of mRNA for COX-2 was evaluated by real-time RT-PCR. Data represent the mean ± S.E. of four separate experiments. *, $p < 0.01$ *versus* the controls. *B*, protein samples were immunoblotted with anti-COX-2 or anti-β-actin antibodies. Data represent three experiments with different cell preparations. *C*, RAW264.7 cells were preincubated with 10 μM NS-398 or 10 μM meloxicam for 1 h (C), and then incubated with 40 μg/ml Ox-LDL for 24 h. PPARα or PPARγ ligand binding activity was determined using the GAL4 chimera system. The data represent the mean ± S.E. of four separate experiments. *, $p < 0.01$ *versus* the controls. †, $p < 0.01$ *versus* cells incubated with Ox-LDL alone. *D* and *E*, RAW264.7 cells were transfected with control or COX-2 siRNA, and then incubated with 40 μg/ml Ox-LDL for 24 h. *D*, protein samples were immunoblotted with anti-COX-2 or anti-β-actin antibodies. Data represent three experiments with different cell preparations. *E*, PPARα or PPARγ ligand binding activity was determined using the GAL4 chimera system. The data represent the mean ± S.E. of four separate experiments. *, $p < 0.01$ *versus* the controls. †, $p < 0.01$ *versus* cells incubated with Ox-LDL alone.

ERK1/2 and p38 MAPK activation in RAW264.7 cells. Ox-LDL (40 μg/ml) transiently increased phosphorylation of ERK1/2 and p38 MAPK at 1 h, which remained for up to 6 h (Fig. 3*A*).

We therefore examined the effect of ERK1/2-specific inhibitor PD98059 and p38 MAPK-specific inhibitor SB203580 on Ox-LDL-induced COX-2 mRNA expression. The incubation of RAW264.7 cells with Ox-LDL for 3 h increased COX-2 mRNA level by 3-fold (Fig. 3*B*), and this increase was blocked by PD98059, but not by SB203580 (Fig. 3*B*). Ox-LDL-induced COX-2 protein expression was also inhibited by PD98059, but not by SB203580 (Fig. 3*C*). In addition, Ox-LDL-induced activation of PPARα and PPARγ was significantly inhibited by PD98059, but not by SB203580 (Fig. 3*D*). Moreover, Ox-LDL-

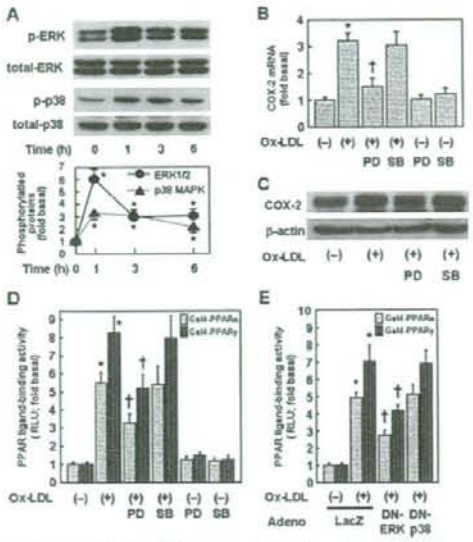

FIGURE 3. **Ox-LDL-induced ERK1/2 activation is involved in COX-2 expression.** *A*, RAW264.7 cells were incubated with 40 μg/ml Ox-LDL for the indicated times. Protein samples were immunoblotted with anti-phospho ERK1/2 (*p-ERK*), anti-ERK1/2 (*total-ERK*), anti-phospho p38 MAPK (*p-p38*) or anti-p38 MAPK (*total-p38*) antibodies. Quantitative results represent the mean ± S.E. of four separate experiments. *, $p < 0.01$ *versus* each pre-stimulated condition (0 min). *B* and *C*, RAW264.7 cells were preincubated with 20 μM PD98059 (*PD*) or 10 μM SB203580 (*SB*) for 1 h, and then with 40 μg/ml Ox-LDL for 3 h (*B*) or 6 h (*C*). COX-2 mRNA expression was evaluated by real-time RT-PCR (*B*) and COX-2 or β-actin protein was detected by Western blot analysis (*C*). Data represent the mean ± S.E. of four separate experiments. *, $p < 0.01$ *versus* the controls. †, $p < 0.01$ *versus* cells incubated with Ox-LDL alone. *D* and *E*, RAW264.7 cells were preincubated with 20 μM PD98059 (*PD*) or 10 μM SB203580 (*SB*) for 1 h (*D*), or infected with dominant-negative ERK (*DN-ERK*), dominant-negative p38 MAPK (*DN-p38*), or LacZ (*E*), and then incubated with 40 μg/ml Ox-LDL for 24 h. PPARα or PPARγ ligand binding activity was determined using the GAL4 chimera system. The data represent the mean ± S.E. of four separate experiments. *, $p < 0.01$ *versus* the controls. †, $p < 0.01$ *versus* cells incubated with Ox-LDL alone.

induced activation of PPARα and PPARγ was also inhibited by overexpression of DN-ERK but not by that of DN-p38 MAPK (Fig. 3*E*). These results suggest that Ox-LDL-induced activation of PPARα and PPARγ activation is mediated by ERK1/2-dependent COX-2 expression.

Ox-LDL Decreases the Amount of Intracellular Long Chain Fatty Acids, but Increases Intracellular 15d-PGJ$_2$ Level—Intracellular fatty acids have been reported to be ligands of PPARα and PPARγ; therefore, we examined the effect of Ox-LDL on the amount of arachidonic acid, oleic acid, linoleic acid, and docosahexaenoic acid. Interestingly, Ox-LDL, but not LDL, significantly decreased all of these fatty acids (Table 2).

It is possible that overexpression of COX-2 may increase the amount of intracellular 15d-PGJ$_2$, which is a natural ligand for PPARγ. Therefore, we examined whether Ox-LDL was capable of increasing 15d-PGJ$_2$ level in macrophages. Ox-LDL (40 μg/ml) significantly increased intracellular 15d-PGJ$_2$ level (Fig. 4*A*), and this was inhibited by PD98059, NS-398, or meloxicam, whereas SB203580 had no such effect (Fig. 4*A*). Moreover, overexpression of DN-ERK (Fig. 4*B*) or transfection of COX-2

TABLE 2
Effect of Ox-LDL on intracellular fatty acids production

RAW264.7 cells were incubated for 24 h with LDL (40 μg/ml) or Ox-LDL (40 μg/ml), and cells were re-suspended by PBS. Intracellular fatty acids were determined by gas chromatography. Data were normalized by cell numbers and represent the mean ± S.E. of four separate experiments.

	Control	Ox-LDL	LDL
Arachidonic acid (μg/ml)	0.77 ± 0.06	0.35 ± 0.03*	0.81 ± 0.04
Oleic acid (μg/ml)	1.58 ± 0.11	0.79 ± 0.08*	1.63 ± 0.12
Linoleic acid (μg/ml)	0.52 ± 0.06	0.23 ± 0.01*	0.57 ± 0.04
Docosahexaenoic acid (μg/ml)	0.55 ± 0.08	0.22 ± 0.02*	0.58 ± 0.05

*$p < 0.01$ *versus* the controls.

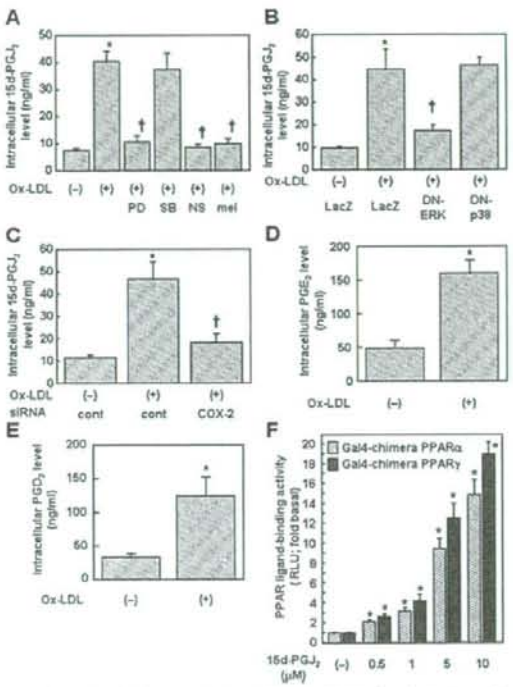

FIGURE 4. **Ox-LDL increases intracellular 15d-PGJ$_2$ level.** *A*, *B*, and *C*, RAW264.7 cells were preincubated with 20 μM PD98059 (*PD*), 10 μM SB203580 (*SB*), 10 μM NS-398 or 10 μM meloxicam for 1 h (*A*), infected with dominant-negative ERK (*DN-ERK*), dominant-negative p38 MAPK (*DN-p38*) or LacZ (*B*), or transfected with siRNA of control or COX-2 (*C*), and then incubated with 40 μg/ml Ox-LDL for 24 h. The concentrations of 15d-PGJ$_2$ were determined by EIA. The data represent the mean ± S.E. of four separate experiments. *, $p < 0.01$ *versus* the controls. †, $p < 0.01$ *versus* cells incubated with Ox-LDL alone. *D* and *E*, RAW264.7 cells were incubated with 40 μg/ml Ox-LDL for 24 h. The concentrations of PGE$_2$ (*D*) or PGD$_2$ (*E*) were determined by EIA. The data represent the mean ± S.E. of four separate experiments. *, $p < 0.01$ *versus* the controls. *F*, RAW264.7 cells were incubated with the indicated concentrations of 15d-PGJ$_2$ for 24 h. PPARα or PPARγ ligand binding activity was determined using the GAL4 chimera system. The data represent the mean ± S.E. of four separate experiments. *, $p < 0.01$ *versus* the controls.

siRNA (Fig. 4*C*) also suppressed Ox-LDL-induced increase in intracellular 15d-PGJ$_2$ level. On the other hand, Ox-LDL (40 μg/ml) significantly increased not only intracellular 15d-PGJ$_2$ level but also intracellular PGE$_2$ (Fig. 4*D*) and PGD$_2$ (Fig. 4*E*).

PPARα activation induced by Ox-LDL was also suppressed by COX-2 inhibition, therefore, we speculated that 15d-PGJ$_2$

TABLE 3
Plasma lipid profile on WT and apoE$^{-/-}$ mice

	Body weight	TC[a]	TG	HDL-C
	g	*mg/dl*	*mg/dl*	*mg/dl*
WT ($n = 10$)	24.4 ± 3.8	65 ± 18	60 ± 22	46 ± 8
apoE$^{-/-}$ ($n = 9$)	25.8 ± 4.2	499 ± 82[b]	55 ± 27	48 ± 6

[a] TC indicates total cholesterol; TG, triglycerides; and HDL-C, HDL cholesterol
[b] $p < 0.01$ *versus* WT group.

would also induce PPARα activation. As shown in Fig. 4*F*, 15d-PGJ_2 induced not only PPARγ activation but also PPARα activation in a dose-dependent manner. Therefore, it seems likely that changes in COX-2-dependent increase in 15d-PGJ_2 level rather than intracellular fatty acids are involved in Ox-LDL-induced activation of PPARα and PPARγ.

On the other hand, the amount of 15d-PGJ_2 in Ox-LDL (0.55 ng/mg of protein) was significantly ($p < 0.01$) lower than that in native LDL (2.3 ng/mg of protein), suggesting that 15d-PGJ_2 contained in Ox-LDL had no effect on PPARα and PPARγ activation.

Expression of COX-2 and 15d-PGJ_2 and Activation of PPARα and PPARγ Were Observed in Atherosclerotic Lesion of apoE$^{-/-}$ Mice—First, we investigated the differentiation of plasma lipid profile between WT and apoE$^{-/-}$ mice of 24 weeks of age fed the normal diet. Plasma TC level on apoE$^{-/-}$ mice was ~7-fold higher than WT mice, whereas plasma TG level and HDL-cholesterol level had no difference (Table 3). We next investigated atherosclerotic lesion formation in apoE$^{-/-}$ and WT mice. As shown in Fig. 5*A*, atherosclerotic lesions stained by oil red O were observed in apoE$^{-/-}$ mice, but not in WT mice. Immunohistochemistry revealed that Ox-LDL was detected in the atherosclerotic lesion of apoE$^{-/-}$ mice and that was co-localized with macrophages (Fig. 5*B*). We further examined the expression of COX-2 and 15d-PGJ_2, and the activation of PPARα and PPARγ in aortic sinus of apoE$^{-/-}$ or WT mice. In comparison to the WT mice, the expression of COX-2 and 15d-PGJ_2 were increased in aortic sinus of apoE$^{-/-}$ mice (Fig. 5, C and *D*). Moreover, the transcription activities of PPARα and PPARγ were also increased in apoE$^{-/-}$ mice by 2.55- and 2.28-fold, respectively (Fig. 5*E*).

Blockade of Either PPARα or PPARγ Inhibits Ox-LDL-induced ABCA1 mRNA Expression—First, to determine the appropriate concentrations of PPARα or PPARγ antagonists, we examined the inhibitory effects of PPARα antagonist GW6471 or PPARγ antagonist T0070907 on Ox-LDL-induced PPARα or PPARγ activation. As shown in Fig. 6*A*, 0.5 μM GW6471 completely inhibited Ox-LDL-induced PPARα ligand binding activation, without affecting PPARγ ligand binding activity. However, 1 μM GW6471 inhibited both PPARα and PPARγ ligand binding activities (Fig. 6*A*). On the other hand, ≥0.01 μM T0070907 completely inhibited Ox-LDL-induced PPARγ ligand binding activity (Fig. 6*B*). Unexpectedly and surprisingly, 1 μM T0070907 increased PPARα ligand binding activity (Fig. 6*B*). These results indicated that the appropriate concentration of GW6471 for the specific inhibition of PPARα was 0.5 μM and that of T0070907 for the specific inhibition of PPARγ was 0.01 μM, therefore, we used these concentrations for the following experiments.

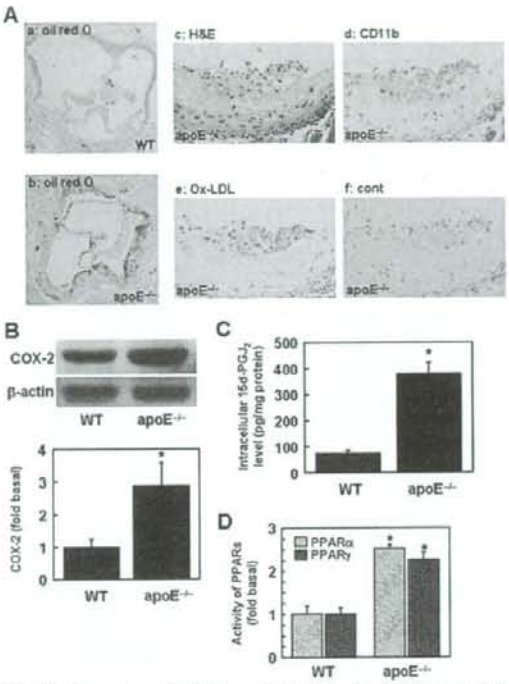

FIGURE 5. **Expression of COX-2 and 15d-PGJ_2 and activation of PPARα and PPARγ in apoE$^{-/-}$ mice aorta.** *A*, representative photographs of atherosclerotic lesions of aortic sinus from WT (*a*) or apoE$^{-/-}$ (*b*, *c*, *d*, *e*, and *f*) mice. *a* and *b*, oil red o; *c*, H&E; *d*, CD11b; *e*, Ox-LDL; *f*, control. Magnification, ×60 (*a* and *b*); ×200 (*c*, *d*, *e*, and *f*). *B–D*, atherosclerotic lesions of aortic sinus were obtained from WT or apoE$^{-/-}$ mice, and COX-2 protein level, 15d-PGJ_2 level and activities of PPARs were determined by Western blot assay (*B*), EIA (*C*), and the assay of transcription activity of PPARs (*D*), respectively. Data represent the mean ± S.E. of five separate experiments. *, $p < 0.01$ *versus* WT mice.

Next, we examined the role of ERK1/2 and COX-2 on Ox-LDL-induced ABCA1 expression. In real-time RT-PCR analysis, 40 μg/ml Ox-LDL significantly induced ABCA1 mRNA expression in mouse peritoneal macrophages (Fig. 6*C*), and the effect was suppressed by NS-398 and PD98059 (Fig. 6*C*). We then examined the role of PPARα and PPARγ activation in Ox-LDL-induced ABCA1 expression. Treatment with 0.5 μM GW6471 or 0.01 μM T0070907 partially, but significantly, inhibited Ox-LDL-induced ABCA1 mRNA expression (Fig. 6*D*). Treatment with both GW6471 and T0070907 showed an additive inhibitory effect on Ox-LDL-induced ABCA1 mRNA expression (Fig. 6*D*).

To confirm the involvement of PPARα and PPARγ in Ox-LDL-induced ABCA1 mRNA expression, the effect of PPARα and/or PPARγ siRNA was examined. As shown in Fig. 6*E*, treatment with siRNA for PPARα and PPARγ, the expression of PPARα and PPARγ, including PPARγ1 and PPARγ2, were suppressed by 72 and 77%, respectively. In comparison to control siRNA, siRNA for PPARα or PPARγ significantly suppressed Ox-LDL-induced ABCA1 mRNA expression (Fig. 6*F*), and an

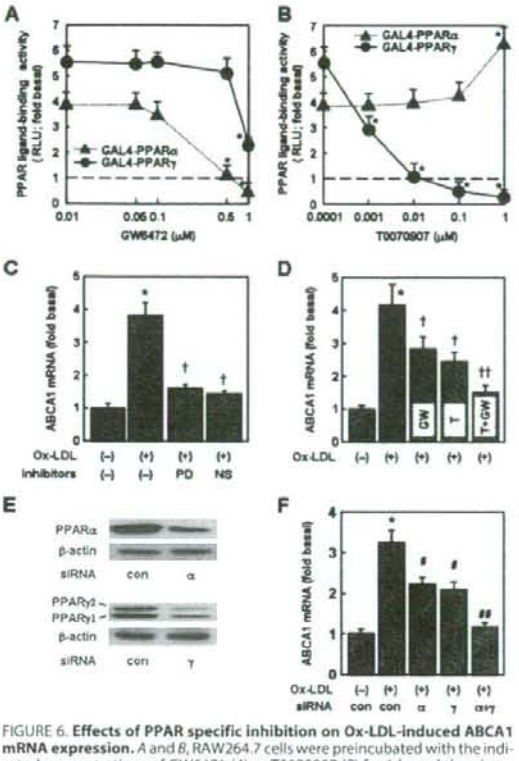

FIGURE 6. **Effects of PPAR specific inhibition on Ox-LDL-induced ABCA1 mRNA expression.** *A* and *B*, RAW264.7 cells were preincubated with the indicated concentrations of GW6471 (*A*) or T0070907 (*B*) for 1 h, and then incubated with 40 μg/ml Ox-LDL for 24 h. PPARα (▲) or PPARγ (●) ligand binding activity was determined using the GAL4 chimera system. *, $p < 0.01$ *versus* cells treated with 0.1 nM T0070907 or 0.01 μM GW6471. *C–F*, mouse peritoneal macrophages were pre-incubated with 20 μM PD98059 (*PD*) or 10 μM NS-398 (*NS*) (*C*), or 10 nM T0070907 (*T*), and/or 0.5 μM GW6471 (*GW*) for 1 h (*D*), or transfected with siRNA of PPARα (α) and/or PPARγ (γ), or control siRNA (*con*) (*E* and *F*), and then incubated with 40 μg/ml Ox-LDL for 24 h. The mRNA expression of ABCA1 was evaluated by real-time RT-PCR (*C*, *D*, and *F*). The expression of PPARα, PPARγ1, and PPARγ2 were detected by Western blot analysis (*E*). Data represent the mean ± S.E. of four separate experiments. *, $p < 0.01$ *versus* the controls. †, $p < 0.01$ *versus* cells incubated with Ox-LDL. ††, $p < 0.01$ *versus* Ox-LDL plus T0070907 or GW6471. #, $p < 0.01$ *versus* Ox-LDL plus control siRNA. ##, $p < 0.01$ *versus* Ox-LDL plus PPARα siRNA or PPARγ siRNA alone.

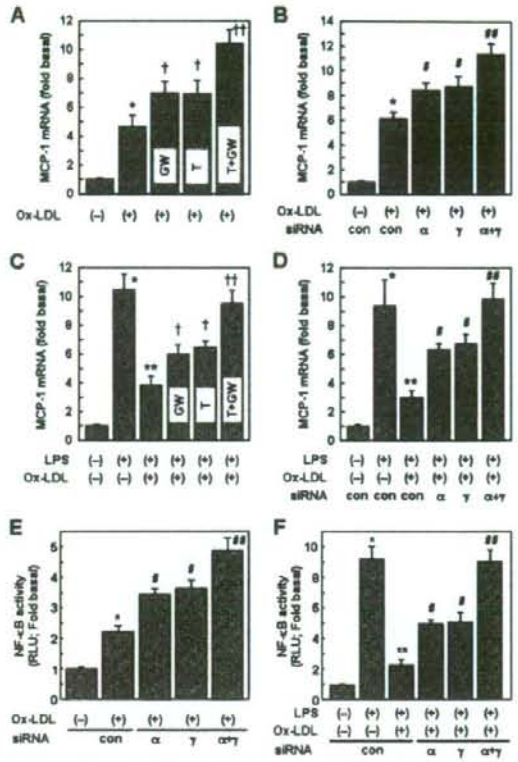

FIGURE 7. **Effects of PPAR-specific inhibition of MCP-1 mRNA expression.** Mouse peritoneal macrophages were preincubated with 10 nM T0070907 (*T*) and/or 0.5 μM GW6471 (*GW*) for 1 h (*A* and *C*), or transfected with siRNA of PPARα (α) and/or PPARγ (γ), or control siRNA (*con*) (*B*, *D*, *E*, and *F*) in the absence (*A–D*) or presence of pNF-κB-Luc (*E* and *F*), and then incubated with 40 μg/ml Ox-LDL in the absence (*A*, *B*, and *E*) or presence (*C*, *D*, and *F*) of 1 μg/ml LPS for 24 h. *A–D*, total RNA was extracted, and the mRNA expression of MCP-1 was evaluated by real-time RT-PCR. *E* and *F*, the activity of NF-κB was determined by luciferase assays. Data represent the mean ± S.E. of four separate experiments. *, $p < 0.01$ *versus* the controls. †, $p < 0.01$ *versus* cells incubated with Ox-LDL alone. ††, $p < 0.01$ *versus* Ox-LDL plus T0070907 or GW6471 alone. #, $p < 0.01$ *versus* Ox-LDL plus control siRNA alone. ##, $p < 0.01$ *versus* Ox-LDL plus PPARα siRNA or PPARγ siRNA alone.

additive effect of siRNA for PPARα and PPARγ was observed (Fig. 6*F*).

PPAR Activation Influences the Two Contrary Effects of Ox-LDL on MCP-1 mRNA Expression—We further examined the effects of PPAR antagonists on Ox-LDL-induced MCP-1 mRNA expression. Ox-LDL (40 μg/ml) increased MCP-1 mRNA expression by 4.7-fold in mouse peritoneal macrophages (Fig. 7*A*). GW6471 or T0070907 significantly enhanced Ox-LDL-induced MCP-1 mRNA expression (Fig. 7*A*), and an additive effect of GW6471 and T0070907 was observed (Fig. 7*A*). Moreover, Ox-LDL-induced MCP-1 mRNA expression was significantly enhanced by siRNA for PPARα or PPARγ (Fig. 7*B*), and an additive effect was observed with combination of siRNAs for PPARα and PPARγ (Fig. 7*B*).

Ox-LDL has also been reported to exert an anti-inflammatory effect in macrophages (33, 34). To clarify the role of PPARα and PPARγ on Ox-LDL-mediated anti-inflammatory effects, we examined the effects of PPARα- and PPARγ-specific inhibition on Ox-LDL-mediated suppression of MCP-1 mRNA expression induced by LPS.

LPS (1 μg/ml) increased MCP-1 mRNA expression by 10.5-fold, which was suppressed by Ox-LDL in mouse peritoneal macrophages (Fig. 7*C*). GW6471 or T0070907 significantly recovered the suppression of MCP-1 mRNA (Fig. 7*C*), and an additive effect of GW6471 and T0070907 was observed (Fig. 7*C*). In addition, in comparison to control siRNA, siRNA for PPARα or PPARγ significantly recovered Ox-LDL-mediated suppression of MCP-1 mRNA (Fig. 7*D*), and an additive effect of PPARα and PPARγ siRNA was observed (Fig. 7*D*).

Ox-LDL Activates PPARs via COX-2 Expression

On the other hand, it has been reported that MCP-1 expression was mediated by the activation of NF-κB (35). Therefore, we examined the effect of Ox-LDL on NF-κB activation. Ox-LDL (40 μg/ml) increased NF-κB activity (Fig. 7*E*). Ox-LDL-induced NF-κB activation was enhanced by treatment of siRNA for PPARα or PPARγ, and an additive effect of PPARα and PPARγ siRNA was observed (Fig. 7*E*). Moreover, LPS (1 μg/ml) induced NF-κB activation, and this activation was inhibited by Ox-LDL (Fig. 7*F*). Treatment with siRNA for PPARα or PPARγ partially recovered Ox-LDL-mediated suppression of NF-κB activation (Fig. 7*F*), and an additive effect of PPARα and PPARγ siRNA was observed (Fig. 7*F*).

DISCUSSION

It has been reported that Ox-LDL induces PPARα and PPARγ activation, and that 9-HODE, 13-HODE, and oxidized phospholipids, which are components of Ox-LDL, are involved in Ox-LDL-induced PPARα and PPARγ activation (12, 14). However, we newly revealed that Ox-LDL-induced PPARα and PPARγ activation was also mediated by overexpression of COX-2. COX-2 is a rate-limiting enzyme of PG synthesis, which catalyzes the conversion of arachidonic acid to PGG_2 and further to PGH_2 (36). It has been reported that Ox-LDL induces COX-2 expression in monocytes/macrophages (37, 38). However, the mechanisms of Ox-LDL-induced COX-2 expression are not clearly understood.

We demonstrated here, possibly for the first time, that Ox-LDL induced COX-2 expression in RAW264.7 macrophages, and that this was mediated by the activation of ERK1/2, but not p38 MAPK. In addition, Ox-LDL-induced activation of PPARα and PPARγ was inhibited by inhibition of COX-2 and ERK1/2, suggesting that Ox-LDL-induced activation of both PPARα and PPARγ is mediated by ERK1/2-dependent COX-2 expression in macrophages. Interestingly, our recent report revealed that statins activated PPARα and PPARγ, and this effect was also mediated by overexpression of COX-2 (11). Thus, several pathways that lead to the overexpression of COX-2 may also induce the activation of PPARα and PPARγ.

In the present study, we demonstrated that siRNA for COX-2 suppressed Ox-LDL-induced COX-2 expression by 86%. However, the siRNA for COX-2 inhibited Ox-LDL-induced PPARα and PPARγ activation by ~50%. Moreover, although inhibitors of COX-2 or ERK1/2 suppressed Ox-LDL-induced increase in 15d-PGJ_2 level by 80% or more, they suppressed PPARα and PPARγ activation by 50%. These results suggest that one or more other mechanisms than COX-2 are involved in Ox-LDL-induced PPARs activation. Because it is reported that 9-HODE, 13-HODE, and oxidized phospholipids, which are included in Ox-LDL, are capable to activate PPARα and PPARγ (12, 14), additive effects by these particles may be involved in Ox-LDL-induced PPARα and PPARγ activation (Fig. 8).

It has been reported that CCAAT/enhancer-binding protein-β (C/EBPβ) and AP-1 are involved in transcriptional activation of the COX-2 gene (39), and MAPK signaling pathways influence AP-1 and C/EBPβ activity (40, 41). Therefore, Ox-LDL-induced ERK1/2 activation may activate AP-1 and/or C/EBPβ, thereby resulting in transcriptional activation of the COX-2 gene. Further studies are needed to clarify the mechanisms by which Ox-LDL induces expression of COX-2 mRNA.

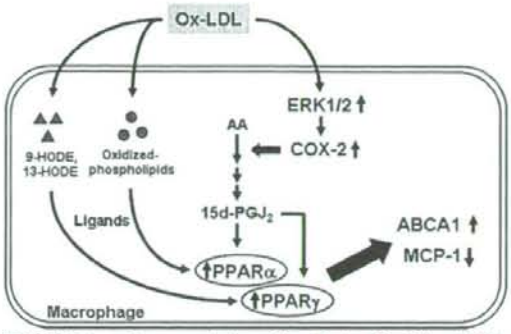

FIGURE 8. **Schematic representation of the effects of Ox-LDL on PPARα and PPARγ activation in macrophages.** The results of the present study revealed the following scheme for the mechanism of Ox-LDL-induced PPARα and PPARγ activation. When macrophages are treated with Ox-LDL, several components of Ox-LDL, such as 9-HODE, 13-HODE, and oxidized phospholipids, work as PPAR ligands, and then PPARα and PPARγ are activated. On the other hand, Ox-LDL also induces ERK1/2-dependent overexpression of COX-2. Overexpression of COX-2 increases intracellular 15d-PGJ_2 level, and finally activates PPARα and PPARγ. The activation of PPARα and PPARγ mediates the up-regulation of ABCA1 mRNA expression and down-regulation of MCP-1 mRNA expression. *AA*, arachidonic acid.

We found that the COX-2 expression induced by Ox-LDL increased the amount of intracellular 15d-PGJ_2. Moreover, Ox-LDL increased not only 15d-PGJ_2 level but also PGE_2 and PGD_2, suggesting that Ox-LDL-induced COX-2-expression mediated the downstream production of prostaglandins. It is well known that 15d-PGJ_2 is a strong PPARγ activator. However, Forman *et al.* (42) have reported that 15d-PGJ_2 is not a PPARα ligand but also activates PPARα. In fact, we demonstrated that 15d-PGJ_2 increased ligand binding activity of both PPARα and PPARγ. These results suggest that COX-2-mediated increase in 15d-PGJ_2 level is one of the mechanisms by which Ox-LDL induces activation of both PPARα and PPARγ.

It has been reported that selective COX-2 inhibition suppresses atherosclerotic lesion formation in LDL receptor-deficient mice (43), suggesting that COX-2 act as an inducer of atherosclerosis. On the other hand, recent studies have revealed that treatment with COX-2 inhibitors in humans does not decrease, but rather increases cardiovascular events (44–46). According to our findings, it is possible that several eicosanoids produced by COX-2 may play a protective role in controlling atherosclerotic progression, through the activation of PPARs.

In the present study, we demonstrated several research activities by *in vitro*. On the other hand, we revealed for the first time that the activities of PPARα and PPARγ were increased in atherosclerotic lesions of apoE$^{-/-}$ mice. We confirm that Ox-LDL was present in these atherosclerotic lesions and that was co-localized with macrophages. Moreover, the expression of COX-2 was also increased in these lesions. In fact, the existence of Ox-LDL and the expression of COX-2 in atherosclerotic lesions have been reported, and these are co-localized with macrophages (43, 47, 48). In addition, we newly found that the

15d-PGJ_2 level was also increased in these atherosclerotic lesions. These results suggested that Ox-LDL activates PPARα and PPARγ *in vivo*, and the effect may be induced by COX-2-dependent 15d-PGJ_2 expression.

ABCA1, a member of the ATP-binding cassette transporter family, is involved in the control of high density lipoprotein and apolipoprotein A1-mediated cholesterol efflux from macrophages (49, 50). The activation of ABCA1 plays an important role by influencing cellular cholesterol transport (51). It has been reported that both PPARα and PPARγ activators induce ABCA1 gene expression in macrophages (52), suggesting that the activation of PPARs leads to anti-atherogenic activity, by the expression of ABCA1 in atherosclerotic lesions. Ox-LDL has been reported to promote uptake of Ox-LDL by inducing the scavenger receptor CD36, via activation of PPARγ in macrophages (14, 53). On the other hand, we demonstrated here, possibly for the first time, that Ox-LDL induced ABCA1 mRNA expression, and this effect was also mediated by PPAR activation. Thus, Ox-LDL-induced activation of PPARs fundamentally accelerates the uptake of Ox-LDL via CD36 expression, and beside this action, Ox-LDL may negatively control the excess accumulation of OX-LDL via ABCA-1 expression.

It has been reported that Ox-LDL induces pro-inflammatory cytokines that are associated with the progression of atherosclerosis (1). On the other hand, in macrophages activated by LPS, Ox-LDL suppresses production of pro-inflammatory cytokines (33, 34), suggesting that Ox-LDL has both inflammatory and anti-inflammatory actions. In fact, in unstimulated conditions, Ox-LDL induces MCP-1 mRNA expression, which is well known to play an early and important role in the recruitment of monocytes to atherosclerotic lesions (54). On the contrary, Ox-LDL inhibited MCP-1 mRNA expression in macrophages activated by LPS. Moreover, Ox-LDL-induced MCP-1 mRNA expression was enhanced by both PPAR-specific inhibitors, and Ox-LDL-mediated suppression of MCP-1 mRNA induced by LPS was recovered by both PPAR-specific inhibitors. Furthermore, like MCP-1, NF-κB, which has been reported to be one of the important molecules in MCP-1 expression (35), was also controlled by Ox-LDL. These results suggest that Ox-LDL can induce MCP-1, whereas the activation of PPARs by Ox-LDL partially suppresses its induction via anti-inflammatory action, such as inactivation of NF-κB, through PPARs.

To confirm whether the ability of Ox-LDL on PPARs activation depended on a degree of its oxidation, we investigated the effect of m-Ox-LDL on PPARα and PPARγ activation. We found that m-Ox-LDL mildly but significantly induced PPARα and PPARγ activation, suggesting that Ox-LDL-induced PPARα and PPARγ activation was depended on its oxidation. Moreover, we found that macrophage-mediated Ox-LDL, whose existence was more realistic than $CuSO_4$-mediated Ox-LDL in atherosclerotic lesions, also activated PPARα and PPARγ. Therefore, it is possible that Ox-LDL activates PPARα and PPARγ in these lesions *in vivo*.

In conclusion, we demonstrated that Ox-LDL-induced PPARα and PPARγ activation was mediated by increase in 15d-PGJ_2, via ERK1/2-dependent COX-2 expression in macrophages. In addition, inhibition of PPARs suppressed Ox-LDL-induced ABCA1 mRNA expression and enhanced Ox-LDL-induced MCP-1 mRNA expression. These unique signals of macrophages induced by Ox-LDL may be one of the protective mechanisms to prevent progression of atherosclerosis. Considering the involvement of COX-2 expression on Ox-LDL-induced activation of PPARs, activation or expression, rather than inhibition of COX-2, may be a novel therapeutic approach for atherosclerosis.

Acknowledgments—We thank Dr. Michael Brownlee (Dept. of Medicine, Diabetes Research Center, Albert Einstein College of Medicine, Bronx, NY) for the generous gifts of $(AOX)^3$-luc and pCMX-PPARγ2 and Dr. Takahide Miyamoto and Dr. Tomoko Kakizawa (Dept. of Aging Medicine and Geriatrics, Shinshu University School of Medicine, Japan) for CMV-hPPARα. We appreciate the helpful advice and assistance of members of the Gene Technology Center (Kumamoto University), as well as Kenshi Ichinose from our laboratory.

REFERENCES

1. Ross, R. (1999) *N. Engl. J. Med.* **340,** 115–126
2. Steinberg, D., Parthasarathy, S., Carew, T. E., Khoo, J. C., and Witztum, J. L. (1989) *N. Engl. J. Med.* **320,** 915–924
3. Lemberger, T., Desvergne, B., and Wahli, W. (1996) *Annu. Rev. Cell Dev. Biol.* **12,** 335–363
4. Kliewer, S. A., Forman, B. M., Blumberg, B., Ong, E. S., Borgmeyer, U., Mangelsdorf, D. J., Umesono, K., and Evans, R. M. (1994) *Proc. Natl. Acad. Sci. U. S. A.* **91,** 7355–7359
5. Braissant, O., Foufelle, F., Scotto, C., Dauca, M., and Wahli, W. (1996) *Endocrinology* **137,** 354–366
6. Tontonoz, P., Hu, E., Graves, R. A., Budavari, A. I., and Spiegelman, B. M. (1994) *Genes Dev.* **8,** 1224–1234
7. Tontonoz, P., Hu, E., and Spiegelman, B. M. (1994) *Cell* **79,** 1147–1156
8. Jones, P. S., Savory, R., Barratt, P., Bell, A. R., Gray, T. J., Jenkins, N. A., Gilbert, D. J., Copeland, N. G., and Bell, D. R. (1995) *Eur. J. Biochem.* **233,** 219–226
9. Li, A. C., Binder, C. J., Gutierrez, A., Brown, K. K., Plotkin, C. R., Pattison, J. W., Valledor, A. F., Davis, R. A., Willson, T. M., Witztum, J. L., Palinski, W., and Glass, C. K. (2004) *J. Clin. Invest.* **114,** 1564–1576
10. Li, A. C., Brown, K. K., Silvestre, M. J., Willson, T. M., Palinski, W., and Glass, C. K. (2000) *J. Clin. Invest.* **106,** 523–531
11. Yano, M., Matsumura, T., Senokuchi, T., Ishii, N., Murata, Y., Taketa, T., Motoshima, H., Taguchi, T., Sonoda, K., Kukidome, D., Takuwa, Y., Kawada, T., Brownlee, M., Nishikawa, T., and Araki, E. (2007) *Circ. Res.* **100,** 1442–1451
12. Lee, H., Shi, W., Tontonoz, P., Wang, S., Subbanagounder, G., Hedrick, C. C., Hama, S., Borromeo, C., Evans, R. M., Berliner, J. A., and Nagy, L. (2000) *Circ. Res.* **87,** 516–521
13. Delerivea, P., Furmana, C., Teissiera, E., Fruchartа, J. C., Durieza, P., and Staels, B. (2000) *FEBS Lett.* **471,** 34–38
14. Nagy, L., Tontonoz, P., Alvarez, J. G., Chen, H., and Evans, R. M. (1998) *Cell* **93,** 229–240
15. Fujiwara, Y., Kiyota, N., Hori, M., Matsushita, S., Iijima, Y., Aoki, K., Shibata, D., Takeya, M., Ikeda, T., Nohara, T., and Nagai, K. (2007) *Arterioscler. Thromb. Vasc. Biol.* **27,** 2400–32406
16. Itabe, H., Takeshima, E., Iwasaki, H., Kimura, J., Yoshida, Y., Imanaka, T., and Takano, T. (1994) *J. Biol. Chem.* **269,** 15274–15279
17. Matsumura, T., Sakai, M., Kobori, S., Biwa, T., Takemura, T., Matsuda, H., Hakamata, H., Horiuchi, S., and Shichiri, M. (1997) *Arterioscler. Thromb. Vasc. Biol.* **17,** 3013–3020
18. Chodakewitz, J. A., Kupper, T. S., and Coleman, D. L. (1988) *J. Immunol.* **140,** 832–836
19. Munker, R., Gasson, J., Ogawa, M., Koeffler, H. P. (1986) *Nature* **323,** 79–82
20. Matsumura, T., Sakai, M., Matsuda, K., Furukawa, N., Kaneko, K., and

Shichiri, M. (1999) *J. Biol. Chem.* **274,** 37665–37672
21. Hakamata, H., Miyazaki, A., Sakai, M., Suginohara, Y., Sakamoto, Y., and Horiuchi, S. (1994) *Arterioscler. Thromb. Vasc. Biol.* **14,** 1860–1865
22. Sakai, M., Miyazaki, A., Sakamoto, Y., Shichiri, M., and Horiuchi, S. (1992) *FEBS Lett.* **314,** 199–202
23. Lindstedt, K. A. (1993) *J. Biol. Chem.* **268,** 7741–7746
24. Nagano, Y., Arai, H., and Kita, T. (1991) *Proc. Natl. Acad. Sci. U. S. A.* **88,** 6457–6461
25. Noble, R. P. (1968) *J. Lipid Res.* **9,** 693–700
26. Senokuchi, T., Matsumura, T., Sakai, M., Yano, M., Taguchi, T., Matsuo, T., Sonoda, K., Kukidome, D., Imoto, K., Nishikawa, T., Kim-Mitsuyama, S., Takuwa, Y., and Araki, E. (2005) *J. Biol. Chem.* **280,** 6627–6633
27. Miyamoto, T., Kaneko, A., Kakizawa, T., Yajima, H., Kamijo, K., Sekine, R., Hiramatsu, K., Nishii, Y., Hashimoto, T., and Hashizume, K. (1997) *J. Biol. Chem.* **272,** 7752–7758
28. Takahashi, N., Kawada, T., Goto, T., Yamamoto, T., Taimatsu, A., Matsui, N., Kimura, K., Saito, M., Hosokawa, M., Miyashita, K., and Fushiki, T. (2002) *FEBS Lett.* **514,** 315–322
29. Matsuo, T., Matsumura, T., Sakai, M., Senokuchi, T., Yano, M., Kiritoshi, S., Sonoda, K., Kukidome, D., Pestell, R. G., Brownlee, M., Nishikawa, T., and Araki, E. (2004) *Biochem. Biophys. Res. Commun.* **314,** 817–823
30. Zhan, Y., Kim, S., Izumi, Y., Izumiya, Y., Nakao, T., Miyazaki, H., and Iwao, H. (2003) *Arterioscler. Thromb. Vasc. Biol.* **23,** 795–801
31. Folch, J., Lees, M., and Sloane Stanley, G. H. (1957) *J. Biol. Chem.* **226,** 497–509
32. Senokuchi, T., Matsumura, T., Sakai, M., Matsuo, T., Yano, M., Kiritoshi, S., Sonoda, K., Kukidome, D., Nishikawa, T., and Araki, E. (2004) *Atherosclerosis* **176,** 233–245
33. Hamilton, T. A., Major, J. A., and Chisolm, G. M. (1995) *J. Clin. Invest.* **95,** 2020–2027
34. Ohlsson, B. G., Englund, M. C., Karlsson, A. L., Knutsen, E., Erixon, C., Skribeck, H., Liu, Y., Bondjers, G., and Wiklund, O. (1996) *J. Clin. Invest.* **98,** 78–89
35. Ueda, A., Ishigatsubo, Y., Okubo, T., and Yoshimura, T. (1997) *J. Biol. Chem.* **272,** 31092–31099
36. Campbell, W. B., and Halushka, P. V. (1996) in *Goodman & Gilman's The Pharmacological Basis of Therapeutics, 9th Edition* (Hardman, J. G., and Limbird, L. E., eds) pp. 601–616, McGraw-Hill, NY
37. Pontsler, A. V., Hilaire, A. S., Marathe, G. K., Zimmerman, G. A., and McIntyre, T. M. (2002) *J. Biol. Chem.* **277,** 13029–13036
38. Claus, R., Fyrnys, B., Deigner, H. P., and Wolf, G. (1996) *Biochemistry* **35,** 4911–4922
39. Wu, K. K., Liou, J. Y., and Cieslik, K. (2005) *Arterioscler. Thromb. Vasc. Biol.* **25,** 679–685
40. Karin, M. (1995) *J. Biol. Chem.* **270,** 16483–16486
41. Hu, J., Roy, S. K., Shapiro, P. S., Rodig, S. R., Reddy, S. P., Platanias, L. C., Schreiber, R. D., and Kalvakolanu, D. V. (2001) *J. Biol. Chem.* **276,** 287–297
42. Forman, B. M., Chen, J., and Evans, R. M. (1997) *Proc. Natl. Acad. Sci. U. S. A.* **94,** 4312–4317
43. Burleigh, M. E., Babaev, V. R., Oates, J. A., Harris, R. C., Gautam, S., Riendeau, D., Marnett, L. J., Morrow, J. D., Fazio, S., and Linton, M. F. (2002) *Circulation* **105,** 1816–1823
44. FitzGerald, G. A. (2004) *N. Engl. J. Med.* **351,** 1709–1711
45. Furberg, C. D., Psaty, B. M., and FitzGerald, G. A. (2005) *Circulation* **111,** 249
46. Wong, D., Wang, M., Cheng, Y., and FitzGerald, G. A. (2005) *Curr. Opin. Pharmacol.* **5,** 204–210
47. Hernández-Presa, M. A., Martín-Ventura, J. L., Ortego, M., Gómez-Hernández, A., Tuñón, J., Hernández-Vargas, B., Blanco-Colio, L. M., Mas, S., Aparicio, C., Ortega, L., Vivanco, F., Gerique, J. G., Diaz, C., Hernández, G., and Egido, J. (2002) *Atherosclerosis* **160,** 49–58
48. Palinski, W., Rosenfeld, M. E., Ylä-Herttuala, S., Gurtner, G. C., Socher, S. S., Butler, S. W., Paethasarathy, S., Carew, T. E., and Steinberg, D. (1998) *Proc. Natl. Acad. Sci. U. S. A.* **86,** 1372–1376
49. Lawn, R. M., Wade, D. P., Garvin, M. R., Wang, X., Schwartz, K., Porter, J. G., Seilhamer, J. J., Vaughan, A. M., and Oram, J. F. (1999) *J. Clin. Invest.* **104,** R25–R31
50. Oram, J. F., Lawn, R. M., Garvin, M. R., and Wade, D. P. (2000) *J. Biol. Chem.* **275,** 34508–34511
51. Oram, J. F., and Vaughan, A. M. (2000) *Curr. Opin. Lipidol.* **11,** 253–260
52. Chinetti, G., Lestavel, S., Bocher, V., Remaley, A. T., Neve, B., Torra, I. P., Teissier, E., Minnich, A., Jaye, M., Duverger, N., Brewer, H. B., Fruchart, J. C., Clavey, V., and Staels, B. (2001) *Nat. Med.* **7,** 53–58
53. Tontonoz, P., Nagy, L., Alvarez, J. G., Thomazy, V. A., and Evans, R. M. (1998) *Cell* **93,** 241–252
54. Charo, I. F., and Taubman, M. B. (2004) *Circ. Res.* **95,** 858–866

Biochemical and Biophysical Research Communications 376 (2008) 434–438

Contents lists available at ScienceDirect

Biochemical and Biophysical Research Communications

journal homepage: www.elsevier.com/locate/ybbrc

Rottlerin activates AMPK possibly through LKB1 in vascular cells and tissues

Kanou Kojima [a], Hiroyuki Motoshima [a,*], Atsuyuki Tsutsumi [a], Motoyuki Igata [a], Takeshi Matsumura [a], Tatsuya Kondo [a], Junji Kawashima [a], Kenshi Ichinose [a], Noboru Furukawa [a], Kouichi Inukai [b], Shigehiro Katayama [b], Barry J. Goldstein [c], Takeshi Nishikawa [a], Kaku Tsuruzoe [a], Eiichi Araki [a]

[a] Department of Metabolic Medicine, Graduate School of Medical Sciences, Kumamoto University, 1-1-1 Honjo, Kumamoto, Japan
[b] Division of Endocrinology and Diabetes, Department of Medicine, Saitama Medical School, Saitama, Japan
[c] Division of Endocrinology, Diabetes and Metabolic Diseases, Department of Medicine, Jefferson Medical College of Thomas Jefferson University, Philadelphia, PA, USA

ARTICLE INFO

Article history:
Received 29 August 2008
Available online 19 September 2008

Keywords:
AMP-activated protein kinase (AMPK)
LKB1
Rottlerin
Protein kinase C (PKC)
PKCδ
Vascular tissues
Vascular smooth muscle cells (VSMCs)

ABSTRACT

AMP-activated protein kinase (AMPK) is a cellular energy sensor involved in multiple cell signaling pathways that has become an attractive therapeutic target for vascular diseases. It is not clear whether rottlerin, an inhibitor of protein kinase Cδ, activates AMPK in vascular cells and tissues. In the present study, we have examined the effect of rottlerin on AMPK in vascular smooth muscle cells (VSMCs) and isolated rabbit aorta. Rottlerin reduced cellular ATP and activated AMPK in VSMCs and rabbit aorta; however, inhibition of PKCδ by three different methods did not activate AMPK. Both VSMCs and rabbit aorta expressed the upstream AMPK kinase LKB1 protein, and rottlerin-induced AMPK activation was decreased in VSMCs by overexpression of dominant-negative LKB1, suggesting that LKB1 is involved in the upstream regulation of AMPK stimulated by rottlerin. These data suggest for the first time that LKB1 mediates rottlerin-induced activation of AMPK in vascular cells and tissues.

Endothelial dysfunction, as well as migration and proliferation of vascular smooth muscle cells (VSMCs) are critical events in the development and progression of atherosclerosis [1]. Protection of normal endothelial function and inhibition of VSMC proliferation have been effective in preventing clinical and experimental vascular diseases [1–3].

AMP-activated protein kinase (AMPK) is a sensor of cellular energy status that is activated by a decrease in cellular ATP levels and coordinates multiple catabolic and anabolic pathways to maintain cellular energy homeostasis [4,5]. Previously, extensive studies on this kinase demonstrated that AMPK is activated by increases in the cellular AMP:ATP ratio caused by metabolic stresses that either interfere with ATP production (e.g., anti-diabetic medicine metformin) or that accelerate ATP consumption (e.g., skeletal muscle contraction). Once activated, AMPK inhibits energy-consuming cellular processes (such as synthesis of cholesterol and fatty acids) and stimulates energy-producing pathways (such as glucose uptake and β-oxidation of fatty acids). Activation of AMPK by the upstream kinase LKB1 has been recently recognized to mediate such diverse cellular responses as the glucose-reducing effect of metformin and growth-suppressive signals in malignant tumors and non-neoplastic cells [4–6]. Therefore, AMPK has been proposed as a therapeutic target for diabetes, obesity and obesity-linked metabolic disorders [5].

AMPK activation also exhibits several salutary effects on vascular function and improves various experimental vascular abnormalities [7–11]. For example, AMPK activation improves endothelial function [7,9] and suppresses VSMC proliferation [10,11]. Thus, one of the possible interventions to achieve both improvement of endothelial function and inhibition of VSMC proliferation might be via activation of AMPK in vascular tissues.

Protein kinase Cδ (PKCδ) has been reported to be activated by elevated glucose condition [12,13], elevated free fatty acid (FFA) levels [12,14], reactive oxygen species (ROS) [15,16], and growth factors including platelet-derived growth factor [16,17], thrombin and Angiotensin II [18]. Most of the above agents considered to be atherogenic factors closely linked to diabetes, metabolic syndrome and atherosclerosis. Indeed, PKCδ activation was observed in diabetic animals [12] and was suggested to involve FFA-induced insulin resistance [14,19]. Inhibition of PKCδ can bring favorable outcomes in several experimental models including reperfusion injury in stroke [20], coronary artery spasm [21] and migration of VSMCs [17,18,22]. These observations indicate that PKCδ may play a critical role in various vascular diseases and that the inhibition of this molecule may be beneficial in these conditions.

Rottlerin, a natural product isolated from *Mallotus phillippinensis*, was described in 1994 as a specific PKCδ inhibitor [23] and has been widely used to suppress PKCδ activity in numerous studies.

* Corresponding author. Fax: +81 96 366 8397.
E-mail address: hmoto@gpo.kumamoto-u.ac.jp (H. Motoshima).

0006-291X/$ - see front matter © 2008 Elsevier Inc. All rights reserved.
doi:10.1016/j.bbrc.2008.09.007

Recent studies demonstrated that the compound inhibits indirectly PKCδ through its mitochondria uncoupling effect [24,25]. Since this reagent may carry both PKCδ-inhibitory and AMPK-activating properties, it is worth being tested as a candidate of therapeutic medicines for vascular disorders linked with diabetes, metabolic syndrome and atherosclerosis. So far, potency of rottlerin to activate AMPK in vascular cells and tissues has not been tested. Therefore, in the present study, we investigated whether rottlerin activates AMPK in VSMCs and isolated rabbit aortas, and report here that rottlerin activates AMPK in vascular cells and tissues possibly through LKB1.

Materials and methods

Materials. ATP assay kit and PKC inhibitors were from Calbiochem (La Jolla, CA). DMEM and Lipofectamine RNAiMAX were from Invitrogen (Kyoto, Japan). Antibodies for β-actin and PKCδ were from Santa Cruz Biotechnology (Santa Cruz, CA). Isoform-specific antibodies for each PKC molecule were from BD biosciences. Antibodies for the phosphorylated forms of AMPK α-subunit (Thr-172) and acetyl-CoA carboxylase (ACC; Ser-79) were from Cell Signaling Technology (Beverly, MA). Aortas from male Japanese white rabbits were purchased from ARK resource Inc (Kumamoto, Japan).

Cell culture and treatment. Human and rabbit aortic SMCs (HASMCs and RASMCs, respectively) were obtained, cultured and used as described previously [10]. LKB1-deficient A549 and HeLa cells were obtained from Japanese Collection of Research Bioresources (Osaka, Japan) and ATCC, respectively. An equal number of cells were seeded. Cells were treated with the indicated concentrations of each reagent (rottlerin or other PKC inhibitors) or vehicle (DMSO) in serum-free DMEM for indicated periods.

Western blots. Western blotting was performed essentially as previously reported [10]. Same amounts of protein was resolved by SDS–polyacrylamide gel electrophoresis (PAGE) and transferred to PVDF membranes and immunoblotting was performed with the indicated antibodies. Following incubation with horseradish peroxidase-conjugated secondary antibodies, proteins were detected with ECL plus kit (Amersham, Piscataway, NJ) according to the manufacturer's instructions. Immunoreactive bands were quantified by NIH image analysis software.

Measurement of intracellular ATP concentrations. After indicated treatment, cells were washed with phosphate-buffered saline (PBS) three times and lysed in a lysis buffer equipped in ATP assay kit [24]. The assay was performed according to manufacturer's instructions. ATP standard curve was prepared using a series of dilutions of ATP stock solution in triplicate and ATP concentration in each sample was estimated using the standard curve.

Experiments using RNA interference. A mixture of small interfering RNAs (siRNAs) against human PKCδ, On-TARGETplus PKCδ siRNA SMARTpool (L-003524; siPKCδ) and the negative control On-TARGETplus siCONTROL Non-targeting pool (D-001810; siNC) were purchased from Dharmacon (Denver, CO). HASMCs seeded at 60–70% confluence on 6-well dishes were transfected without siRNA (for transfection control experiments) or with siPKCδ or siNC using Lipofectamine RNAiMAX according to the instruction supplied by Invitrogen. After 48 h, cells were then subjected to the indicated experiments.

Experiments using adenoviruses. Adenoviral vectors expressing dominant negative (DN)- and wild type (WT)-LKB1 [26] were used as described previously [10]. An adenoviral vector expressing green fluorescence protein (GFP) was used for the infection control experiments. 3 days after adenoviral infection, HASMCs were treated with rottlerin as indicated.

Statistical analysis. Data were expressed as the means ± SD. Differences between groups were examined for statistical significance by one-factor ANOVA. $p < 0.05$ was considered to indicate a statistically significant difference.

Results

Rottlerin activates AMPK in vascular smooth muscle cells

The impact of rottlerin on AMPK was investigated in human VSMCs. In a dose-dependent manner, treatment with rottlerin for 2 h increased Thr-172 phosphorylation of AMPK, indicative of AMPK activation (Fig. 1A). The enzymatic activation of AMPK was also confirmed by examining Ser-79 phosphorylation of ACC, a major downstream target protein in the AMPK signaling cascade. Consistent with AMPK phosphorylation and activation, phosphorylation of ACC was elevated in rottlerin-treated HASMCs (Fig. 1A). We further investigated the time course of the effect of rottlerin on phosphorylation of AMPK and ACC. AMPK phosphorylation by rottlerin was sustained over 24 h in HASMCs (Fig. 1B). In rabbit VSMCs, similar effects of rottlerin on these molecules were observed (Fig. 1C). Next, we investigated the effect in isolated rabbit aortas. Rottlerin activated AMPK in aortic strips (Fig. 4A). These results indicate that rottlerin activates AMPK and regulates its downstream pathways in primary-cultured VSMCs and vascular tissues.

Rottlerin reduced cellular ATP concentrations in HASMCs

A decrease in cellular ATP causes AMPK activation in many mammalian cells [4–6]. To investigate the mechanism of rottlerin-induced AMPK activation, we measured intracellular ATP concentrations in vehicle- and rottlerin-treated HASMCs. Rottlerin significantly reduced intracellular ATP concentrations within 2 h (Fig. 2A). The effect of rottlerin on cellular ATP was dose-dependent and sustained for at least 24 h (Fig. 2A and B). ATP concentration in rabbit aortic strips treated with 5 μM rottlerin was also decreased (72 ± 8.4% of vehicle-treated, $n = 3$ each). These results suggest that rottlerin may decrease cellular ATP through the inhibition of mitochondrial ATP production as previously reported [24,25], resulting in AMPK activation in HASMCs and isolated aortas.

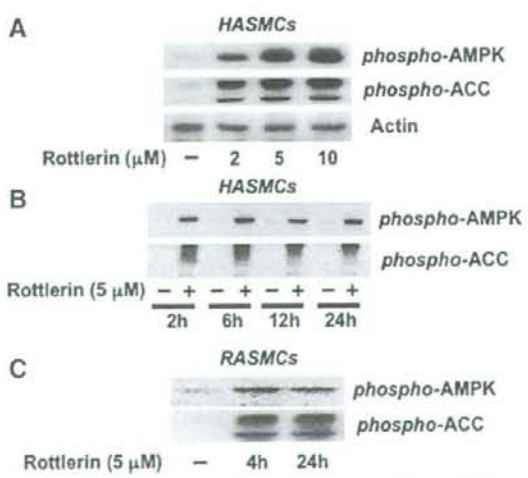

Fig. 1. Rottlerin activates AMPK in HASMCs (A and B) and RASMCs (C). VSMCs were treated with the indicated concentrations of rottlerin or vehicle (–) for 2 h (A) or for indicated periods (B and C). Representative immunoblots of more than three independent experiments are shown.

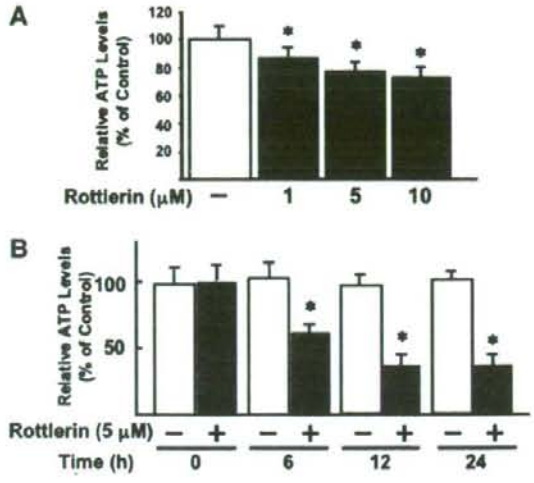

Fig. 2. Rottlerin reduces intracellular ATP in VSMCs. HASMCs (A and B) were treated with indicated concentrations of rottlerin (solid bars) or vehicle (open bars) for 2 h (A) or for indicated periods (B) and then intracellular ATP concentrations were estimated. Each bar represents means ± SD from three independent experiments and relative ATP content compared with values from control experiments incubated with vehicle. $^{*}p < 0.05$ as compared with vehicle treated.

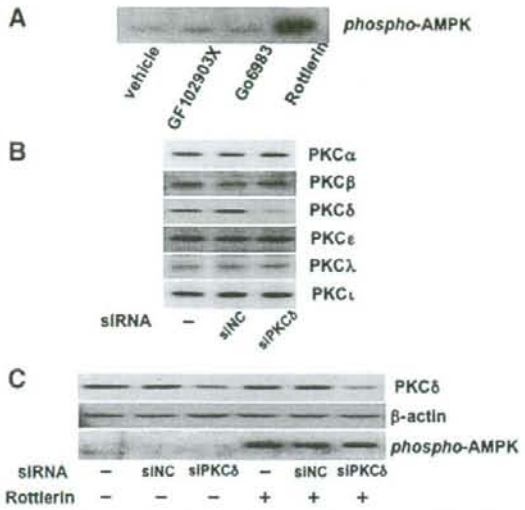

Fig. 3. Inhibitions of PKCδ with different strategies do not activate AMPK. HASMCs were treated with indicated concentrations of GF102903X (1 μM), Go9683 (1 μM), rottlerin (5 μM) or vehicle for 2 h (A). HASMCs were transfected without siRNA (–) or with siPKCδ or the control siNC (B and C). After 48 h, the cells were treated with 5 μM rottlerin or vehicle (–) for 2 h. Western blot analyses were performed to confirm siRNA-mediated gene knockdown (B) and to observe AMPK activation (C). Representative blots from three independent experiments are shown.

Inhibitions of PKCδ do not activate AMPK

Since rottlerin has been reported to be a selective inhibitor of PKCδ, we tested whether an inhibition of PKCδ activity causes AMPK activation in VSMCs. Inhibitions of PKCδ using broad PKC inhibitors GF102903X and Go6983 (at 1 μM) did not cause AMPK phosphorylation (Fig. 3A). Reduction of PKCδ expression by prolonged PMA treatment also had no effect on AMPK phosphorylation (data not shown). To inhibit PKCδ more specifically, we used siRNA-mediated ablation of PKCδ expression. As expected, PKCδ expression reduced by more than 80% after cells were transfected with a mixture of siRNAs against PKCδ (siPKCδ) but not with negative control siRNAs (siNC), and the effect of siPKCδ transfection was specific to PKCδ molecule (Fig. 3B and C). However, inhibition of PKCδ with siPKCδ did not cause AMPK activation (Fig. 3C). Rottlerin consistently activated AMPK in HASMCs transfected with either siPKCδ, siNC or without siRNA (Fig. 3C). These results strongly suggest that rottlerin activates AMPK independent of PKCδ-inhibition.

LKB1 is important for rottlerin-induced AMPK activation

Involvement of LKB1 in AMPK activation has been suggested [4–6,27], however, the presence of LKB1 and a link between LKB1 and AMPK in VSMCs is largely unknown. To investigate this possibility, we treated HASMCs, rabbit aortas and two LKB1-deficient cell lines A549 and HeLa cells with rottlerin and investigated the expression of LKB1 protein and phosphorylation of AMPK and ACC. In HASMCs and rabbit aortas, LKB1 protein was detected with a corresponding molecular size. On the other hand, LKB1 protein was not detected at all in A549 and HeLa cells (Fig. 4A). Rottlerin-induced phosphorylation of AMPK and ACC was observed in HASMCs and rabbit aortas, but not in LKB1-deficient A549 and HeLa cells (Fig. 4A). Next, we introduced WT-LKB1 protein into HeLa cells and investigated the effect on AMPK activation. Without rottlerin, exogenous LKB1 expression caused AMPK activation in HeLa cells. Rottlerin further increased the activation of AMPK in these cells (Fig. 4B). Finally, we overexpressed DN-LKB1 into HASMCs and investigated the effect on AMPK activation by rottlerin. Rottlerin-induced phosphorylation of AMPK and ACC significantly decreased in HASMCs overexpressing DN-LKB1 (32.8% inhibition for AMPK ($p < 0.05$) and 55.5% inhibition for ACC ($p < 0.05$), respectively, compared with those in GFP-infected control HASMCs) (Fig. 4C). These results suggest that LKB1 phosphorylates and activates AMPK in vascular cells and tissues.

Discussion

Although widely thought to be a selective PKCδ inhibitor, we show in the current study that rottlerin is an AMPK activator in human and rabbit VSMCs as well as in isolated rabbit aortic strips. These findings are important because more studies using PKCδ inhibitors to characterize the cellular and physiological effects of this important signaling kinase are appearing in the literature. AMPK activation by rottlerin was also found to be associated with a reduction of cellular ATP levels. Since a decrease of cellular ATP by rottlerin was previously reported [24,25] and reduction of cellular ATP is one of the major mechanisms for AMPK activation [4–6], AMPK activation in vascular cells and tissues by this reagent was not surprising. Indeed, a previous study reported the activation of AMPK by 10 μM of rottlerin in several types of cultured cells [28]. In the manuscript, however, non-vascular cells were used and treated with rottlerin (only at 10 μM), and the effect of inhibition of PKCδ on AMPK activation and the effect of rottlerin in LKB1-deficient cells were not investigated.

In the present study, AMPK phosphorylation in VSMCs by rottlerin was observed from 0.5 to 20 μM (data not shown) and increased in a does-dependent manner. We estimated that the EC_{50} for AMPK phosphorylation was 1.4 and 1.6 μM in HASMCs and RASMCs, respectively (data not shown). These values are clearly lower than the reported IC_{50} of rottlerin for PKCδ (3–6 μM) [23], suggesting that rottlerin affects the AMPK pathway at concentrations that may not inhibit PKCδ. Since rottlerin can inhibit PKCδ

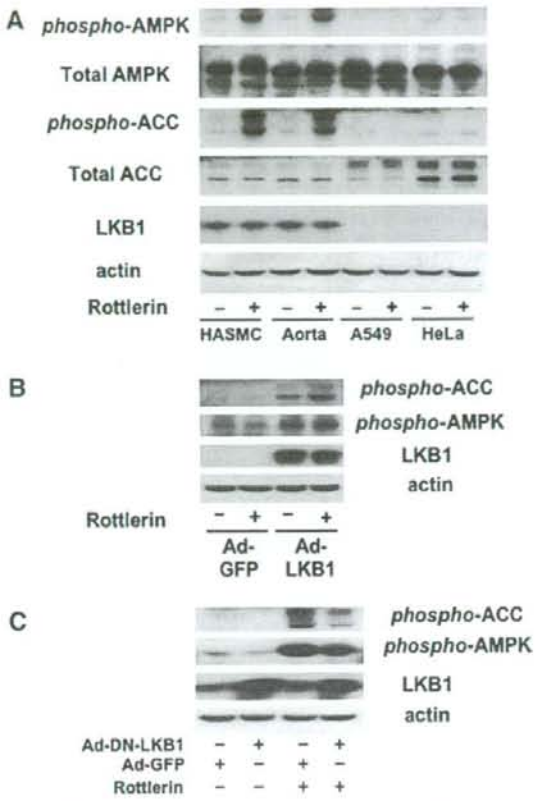

Fig. 4. LKB1 mediates AMPK activation by rottlerin in LKB1-deficient cells and HASMCs. (A) HASMCs, isolated rabbit aortas, or LKB1-deficient cells were treated with 5 μM rottlerin or vehicle for 2 h. (B) HeLa cells infected with adenovirus coding WT-LKB1 were treated with 5 μM rottlerin for 2 h. (C) HASMCs infected with adenovirus coding DN-LKB1 were treated with 5 μM rottlerin for 2 h. Protein expression of LKB1 and phosphorylation of AMPK and ACC were investigated. Representative blots from three independent experiments are shown.

activity in living cells [15,24,25,29] and *in vivo* [30], it is possible that rottlerin may activate AMPK through its PKCδ-inhibitory action. Therefore, we also investigated whether inhibitions of PKCδ cause AMPK activation in HASMCs using three different methods. First, PKCδ-inhibition by two general PKC inhibitors did not cause AMPK activation. Second, down-regulation of PKCδ protein expression by prolonged treatment with PMA did not activate AMPK. Third, more specific PKCδ-inhibition by siRNA did not cause AMPK activation. We have confirmed that rottlerin consistently activated AMPK in PKCδ-downregulated HASMCs with siPKCδ transfection. These observations clearly indicate that AMPK activation by rottlerin is independent of its inhibitory action on PKCδ.

In contrast to VSMCs and rabbit aortas, rottlerin-induced AMPK activation was not observed in two LKB1-deficient cell models. The expression of LKB1 protein of appropriate molecular size was confirmed in HASMCs and rabbit aortas, but not in LKB1-deficient cells. As expected, overexpression of DN-LKB1 in HASMCs significantly suppressed rottlerin-induced phosphorylation of AMPK and ACC. These findings suggest that rottlerin phosphorylates and activates AMPK and regulates its downstream molecules through LKB1 as in the case of phenformin [27]. In addition, to our best knowledge, the present work is the first to demonstrate expression of LKB1 protein in VSMCs. Furthermore, since AMPK activation is expected to cause strong suppression of protein synthesis through inactivation of eEF2 and mTOR, rottlerin treatment may suppress VSMC hypertrophy and proliferation as seen in response to AICAR in cardiac myocytes and VSMCs [10,11,31].

Along with another group [11], we reported that AMPK activation by AICAR strongly inhibits VSMC proliferation [10], and this effect was associated with AMPK-mediated inhibition of neointimal formation induced by balloon-injury *in vivo* [11]. Thus, AMPK activation in VSMCs may be a therapeutic target for vascular proliferative diseases [3,6]. In addition to the growth-inhibitory effect in VSMCs, AMPK activation in vascular system has recently been shown to potentially prevent and treat vascular diseases. For instance, α-lipoic acids prevented endothelial dysfunction and a red wine polyphenol inhibited atherosclerosis through AMPK [7,8]. AMPK is involved in endothelial nitric oxide production in response to shear stress [32] and adiponectin activated AMPK with vascular protective properties [9,33]. According to these reports, rottlerin might confer vascular protection through its action on endothelial AMPK although further investigations *in vivo* are required.

Since rottlerin inhibited PKCδ activity *in vivo* [30], rottlerin may improve vascular abnormalities resulted from elevated PKCδ activity [12]. In most studies that used rottlerin, authors concluded that its beneficial effects of this compound (such as inhibitory effects on cell proliferation and ROS production) might be due to its PKCδ-inhibitory action [15,29,30]. However, it will be of interest in further studies to investigate whether the reported beneficial effects of rottlerin result from signaling effects on AMPK activation vs. PKCδ-inhibition, especially in pathological settings like reperfusion injury, coronary artery spasm and VSMC migration. Furthermore, since some AMPK activators are known to be beneficial for diabetes and obesity-linked disorders in that they stimulate glucose uptake and fatty acid oxidation in skeletal muscles as well as inhibit hepatic gluconeogenesis [5], it will be important to test whether rottlerin has similar metabolic effects.

In conclusion, rottlerin activated AMPK and regulated downstream signaling in vascular cells and tissues, through LKB1. This study provides insight into the role of LKB1 to activate AMPK in primary VSMCs and isolated rabbit aorta and the mechanism of rottlerin as an AMPK activator in this process. Investigators who use this compound in cellular experiments should take into consideration of its action on AMPK and its effects on reducing ATP.

Acknowledgments

This work was supported by a Grant-in-Aid for Scientific Research from Japan Society for the Promotion of Science, Japan (Nos. 16046219 to E. A. and 18590995 to T. N.) and by grant from the Japan Diabetes Foundation (to H.M.).

References

[1] R. Ross, Atherosclerosis—an inflammatory disease, N. Engl. J. Med. 340 (1999) 115–126.
[2] H. Morawietz, S. Erbs, J. Holtz, A. Schubert, M. Krekler, W. Goettsch, O. Kuss, V. Adams, K. Lenk, F.W. Mohr, et al., AT1 blockade and cholesterol-dependent oxidative stress: the EPAS trial, Circulation 114 (2006) 1296–1301.
[3] V.J. Dzau1, R.C. Braun-Dullaeus, D.G. Sedding, Vascular proliferation and atherosclerosis: new perspectives and therapeutic strategies, Nat. Med. 8 (2002) 1249–1256.
[4] D.G. Hardie, New roles for the LKB1 → AMPK pathway, Curr. Opin. Cell Biol. 17 (2005) 167–173.
[5] D.G. Hardie, AMP-activated protein kinase as a drug target, Annu. Rev. Pharmacol. Toxicol. 47 (2007) 185–210.
[6] H. Motoshima, B.J. Goldstein, M. Igata, E. Araki, AMPK and cell proliferation—AMPK as a therapeutic target for atherosclerosis and cancer, J. Physiol. 574 (2006) 63–71.
[7] W.J. Lee, I.K. Lee, H.S. Kim, Y.M. Kim, E.H. Koh, J.C. Won, S.M. Han, M.S. Kim, I. Jo, G.T. Oh, I.S. Park, J.H. Youn, S.W. Park, K.U. Lee, J.Y. Park, α-Lipoic acid prevents

endothelial dysfunction in obese rats via activation of AMP-activated protein kinase, Arterioscler. Thromb. Vasc. Biol. 25 (2005) 2488–2494.
[8] M. Zang, S. Xu, K.A. Maitland-Toolan, A. Zuccollo, X. Hou, B. Jiang, M. Wierzbicki, T.J. Verbeuren, R.A. Cohen, Polyphenols stimulate AMP-activated protein kinase, lower lipids, and inhibit accelerated atherosclerosis in diabetic LDL receptor-deficient mice, Diabetes 55 (2006) 2180–2191.
[9] T. Yamauchi, K. Hara, N. Kubota, Y. Terauchi, K. Tobe, P. Froguel, R. Nagai, T. Kadowaki, Dual roles of adiponectin/Acrp30 in vivo as an anti-diabetic and anti-atherogenic adipokine, Curr. Drug Targets Immune. Endocr. Metabol. Disord. 3 (2003) 243–254.
[10] M. Igata, H. Motoshima, K. Tsuruzoe, K. Kojima, T. Matsumura, T. Kondo, T. Taguchi, K. Nakamaru, M. Yano, D. Kukidome, K. Matsumoto, T. Toyonaga, T. Asano, T. Nishikawa, E. Araki, Adenosine monophosphate-activated protein kinase suppresses vascular smooth muscle cell proliferation through the inhibition of cell cycle progression, Circ. Res. 97 (2005) 837–844.
[11] D. Nagata, R. Takeda, M. Sata, H. Satonaka, E. Suzuki, T. Nagano, Y. Hirata, AMP-activated protein kinase inhibits angiotensin II-stimulated vascular smooth muscle proliferation, Circulation 110 (2004) 444–451.
[12] C. Rask-Madsen, G.L. King, Proatherosclerotic mechanisms involving protein kinase C in diabetes and insulin resistance, Arterioscler. Thromb. Vasc. Biol. 25 (2005) 487–496.
[13] K.V. Ramana, B. Friedrich, R. Tammali, M.B. West, A. Bhatnagar, K. Satish, S.K. Srivastava, Requirement of aldose reductase for the hyperglycemic activation of protein kinase C and formation of diacylglycerol in vascular smooth muscle cells, Diabetes 54 (2005) 818–829.
[14] T.K. Lam, H. Yoshii, C.A. Haber, E. Bogdanovic, L.I. Lam, I.G. Fantus, A. Giacca, Free fatty acid-induced hepatic insulin resistance: a potential role for protein kinase C-δ, Am. J. Physiol. Endocrinol. Metab. 283 (2002) E682–691.
[15] I. Talior, T. Tennenbaum, T. Kuroki, H. Eldar-Finkelman, PKC-δ-dependent activation of oxidative stress in adipocytes of obese and insulin-resistant mice: role for NADPH oxidase, Am. J. Physiol. Endocrinol. Metab. 288 (2005) E405–E411.
[16] S.F. Steinberg, Distinctive activation mechanisms and functions for protein kinase C-δ, Biochem. J. 384 (2004) 449–459.
[17] H. Yamaguchi, M. Igarashi, A. Hirata, N. Sugae, H. Tsuchiya, Y. Jimbu, M. Tominaga, T. Kato, Altered PDGF-BB-induced p38 MAP kinase activation in diabetic vascular smooth muscle cells: roles of protein kinase C-δ, Arterioscler. Thromb. Vasc. Biol. 24 (2004) 2095–2101.
[18] H. Ohtsu, M. Mifune, G.D. Frank, S. Saito, T. Inagami, S. Kim-Mitsuyama, Y. Takuwa, T. Sasaki, J.D. Rothstein, H. Suzuki, H. Nakashima, E.A. Woolfolk, E.D. Motley, S. Eguchi, Signal-crosstalk between Rho/ROCK and c-Jun NH2-terminal kinase mediates migration of vascular smooth muscle cells stimulated by angiotensin II, Arterioscler. Thromb. Vasc. Biol. 25 (2005) 1831–1836.
[19] T.K. Lam, A. Carpentier, G.F. Lewis, G. van de Werve, I.G. Fantus, A. Giacca, Mechanisms of the free fatty acid-induced increase in hepatic glucose production, Am. J. Physiol. Endocrinol. Metab. 284 (2003) E863–E873.
[20] W.H. Chou, R.O. Messing, Protein kinase C isozymes in stroke, Trends Cardiovasc. Med. 15 (2005) 47–51.
[21] T. Kandahashi, H. Shimokawa, K. Miyata, I. Kunihiro, Y. Eto, K. Morishige, Y. Matsumoto, K. Obara, K. Nakayama, S. Takahashi, A. Takeshita, Evidence for protein kinase C-mediated activation of Rho-kinase in a porcine model of coronary artery spasm, Arterioscler. Thromb. Vasc. Biol. 23 (2003) 2209–2214.
[22] C. Li, F. Wernig, M. Leitges, Y. Hu, Q. Xu, Mechanical stress-activated PKCδ regulates smooth muscle cell migration, FASEB J. 17 (2003) 2106–2118.
[23] M. Gschwendt, H.J. Muller, K. Kielbassa, R. Zang, W. Kittstein, G. Rincke, F. Marks, Rottlerin, a novel protein kinase inhibitor, Biochem. Biophys. Res. Commun. 199 (1994) 93–98.
[24] S.P. Soltoff, Rottlerin is a mitochondrial uncoupler that decreases cellular ATP levels and indirectly blocks protein kinase C-δ tyrosine phosphorylation, J. Biol. Chem. 276 (2001) 37986–37992.
[25] J.A. Tapia, R.T. Jensen, L.J. Garcia-Marin, Rottlerin inhibits stimulated enzymatic secretion and several intracellular signaling transduction pathways in pancreatic acinar cells by a non-PKC-δ-dependent mechanism, Biochim. Biophys. Acta 1763 (2006) 25–38.
[26] K. Imai, K. Inukai, Y. Ikegami, T. Awata, S. Katayama, LKB1, an upstream AMPK kinase, regulates glucose and lipid metabolism in cultured liver and muscle cells, Biochem. Biophys. Res. Commun. 351 (2006) 595–601.
[27] K. Sakamoto, O. Goransson, D.G. Hardie, D.R. Alessi, Activity of LKB1 and AMPK-related kinases in skeletal muscle: effects of contraction, phenformin, and AICAR, Am. J. Physiol. Endocrinol. Metab. 287 (2004) E310–E317.
[28] K. Inoki, T. Zhu, K. Guan, TSC2 mediates cellular energy response to control cell growth and survival, Cell 115 (2003) 577–590.
[29] K. Kitamura, K. Mizuno, A. Etoh, Y. Akita, A. Miyamoto, K. Nakayama, S. Ohno, The second phase activation of protein kinase C-δ at late G1 is required for DNA synthesis in serum-induced cell cycle progression, Genes Cells 8 (2003) 311–324.
[30] D. Zhang, V. Anantharam, A. Kanthasamy, A.G. Kanthasamy, Neuroprotective effect of protein kinase C-δ inhibitor rottlerin in cell culture and animal models of Parkinson's disease, J. Pharmacol. Exp. Ther. 322 (2007) 913–922.
[31] A.Y. Chan, C.L. Soltys, M.E. Young, C.G. Proud, J.R. Dyck, Activation of AMP-activated protein kinase inhibits protein synthesis associated with hypertrophy in the cardiac myocytes, J. Biol. Chem. 279 (2004) 32771–32779.
[32] Y. Zhang, T.S. Lee, E.M. Kolb, K. Sun, X. Lu, F.M. Sladek, G.S. Kassab, T. Garland, Y.J. John, J.Y. Shyy, AMP-activated protein kinase is involved in endothelial NO synthase activation in response to shear stress, Arterioscler. Thromb. Vasc. Biol. 26 (2006) 1281–1287.
[33] H. Motoshima, X. Wu, K. Mahadev, B.J. Goldstein, Adiponectin suppresses proliferation and superoxide generation and enhances eNOS activity in endothelial cells treated with oxidized LDL, Biochem. Biophys. Res. Commun. 315 (2004) 264–271.

J Hum Genet (2008) 53:546–553
DOI 10.1007/s10038-008-0283-1

ORIGINAL ARTICLE

Variations in the *FTO* gene are associated with severe obesity in the Japanese

Kikuko Hotta · Yoshio Nakata · Tomoaki Matsuo · Seika Kamohara · Kazuaki Kotani · Ryoya Komatsu · Naoto Itoh · Ikuo Mineo · Jun Wada · Hiroaki Masuzaki · Masato Yoneda · Atsushi Nakajima · Shigeru Miyazaki · Katsuto Tokunaga · Manabu Kawamoto · Tohru Funahashi · Kazuyuki Hamaguchi · Kentaro Yamada · Toshiaki Hanafusa · Shinichi Oikawa · Hironobu Yoshimatsu · Kazuwa Nakao · Toshiie Sakata · Yuji Matsuzawa · Kiyoji Tanaka · Naoyuki Kamatani · Yusuke Nakamura

Received: 22 January 2008 / Accepted: 9 March 2008 / Published online: 1 April 2008

Abstract Variations in the fat-mass and obesity-associated gene (*FTO*) are associated with the obesity phenotype in many Caucasian populations. This association with the obesity phenotype is not clear in the Japanese. To investigate the relationship between the *FTO* gene and obesity in the Japanese, we genotyped single nucleotide polymorphisms (SNPs) in the *FTO* genes from severely obese subjects [$n = 927$, body mass index (BMI) ≥ 30 kg/m^2] and normal-weight control subjects ($n = 1{,}527$, BMI < 25 kg/m^2). A case-control association analysis revealed that 15 SNPs, including rs9939609 and rs1121980, in a linkage disequilibrium (LD) block of approximately 50 kb demonstrated significant associations with obesity; rs1558902 was most significantly associated with obesity. *P* value in additive mode was 0.0000041, and odds ratio (OR) adjusted for age and gender was 1.41 [95% confidential interval (CI) = 1.22–1.62]. Obesity-associated phenotypes, which include the level of plasma glucose, hemoglobin A1c, total cholesterol, triglycerides, high-density lipoprotein (HDL) cholesterol, and blood pressure were not associated with the

Electronic supplementary material The online version of this article (doi:10.1007/s10038-008-0283-1) contains supplementary material, which is available to authorized users.

K. Hotta (✉)
Laboratory for Obesity, SNP Research Center,
RIKEN, 1-7-22 Suehiro, Tsurumi-ku, Yokohama,
Kanagawa 230-0045, Japan
e-mail: kikuko@src.riken.jp

Y. Nakata · T. Matsuo · K. Tanaka
Institute of Health and Sport Sciences,
University of Tsukuba, Ibaraki, Japan

S. Kamohara
Medicine and Health Science Institute,
Tokyo Medical University, Tokyo, Japan

K. Kotani · T. Funahashi · Y. Matsuzawa
Department of Metabolic Medicine,
Graduate School of Medicine, Osaka University, Osaka, Japan

R. Komatsu
Rinku General Medical Center, Osaka, Japan

N. Itoh
Toyonaka Municipal Hospital, Osaka, Japan

I. Mineo
Otemae Hospital, Osaka, Japan

J. Wada
Department of Medicine and Clinical Science,
Okayama University Graduate School of Medicine
and Dentistry, Okayama, Japan

H. Masuzaki · K. Nakao
Department of Medicine and Clinical Science,
Kyoto University Graduate School of Medicine,
Kyoto, Japan

M. Yoneda · A. Nakajima
Division of Gastroenterology, Yokohama City University
Graduate School of Medicine, Yokohama, Japan

S. Miyazaki
Tokyo Postal Services Agency Hospital,
Tokyo, Japan

K. Tokunaga
Itami City Hospital, Hyogo, Japan

M. Kawamoto · N. Kamatani
Institute of Rheumatology, Tokyo Women's Medical University,
Tokyo, Japan

rs1558902 genotype. Thus, the SNPs in the *FTO* gene were found to be associated with obesity, i.e., severe obesity, in the Japanese.

Keywords Fat-mass and obesity-associated gene · Obesity · Japanese population · Association · SNP

Introduction

Obesity is the most common nutritional disorder in developed countries, and it is a major risk factor for hypertension, cardiovascular disease, and type 2 diabetes (Kopelman 2000; Wilson et al. 2003). Genetic and environmental factors contribute to obesity development (Maes et al. 1997; Barsh et al. 2000; Rankinen et al. 2006). Recent progress in single nucleotide polymorphism (SNP) genotyping techniques has enabled genome-wide association studies on common diseases (Herbert et al. 2006; Frayling et al. 2007; Scuteri et al. 2007; The Wellcome Trust Case Control Consortium 2007; Hinney et al. 2007). Using a large-scale case-control association study, we found that secretogranin III (SCG3) (Tanabe et al. 2007) and myotubularin-related protein 9 (MTMR9) (Yanagiya et al. 2007) are involved in susceptibility to the obesity phenotype. Genome-wide association studies have shown that the fat-mass and obesity-associated gene (*FTO*) is also associated with the obesity phenotype (Frayling et al. 2007; Scuteri et al. 2007; Hinney et al. 2007). This association was also found in many Caucasian and Hispanic American populations (Frayling et al. 2007; Scuteri et al. 2007; Dina et al. 2007; Field et al. 2007; Andreasen et al. 2008; Wåhlén et al. 2008; Peeters et al. 2008), whereas it was not found in the Chinese Han population (Li et al. 2008). Among Japanese, body mass index (BMI) was higher in subjects who had the A allele of rs9939609, similar to that observed in Caucasians; however, this finding was not significant (Horikoshi et al. 2007). Another group reported that rs9939609 was associated with BMI in the Japanese (Omori et al. 2008). Thus, the association of SNPs in the *FTO* gene with obesity in the Japanese remains controversial.

To investigate the relationship between the *FTO* gene and obesity in the Japanese, we performed a case-control association study using patients with severe adult obesity (BMI $\geq$ 30 kg/m^2) and normal-weight controls (BMI $<$ 25 kg/m^2); we found that SNPs in intron 1 of the *FTO* gene were associated with severe adult obesity.

Materials and methods

Study subjects

The sample size for severely obese Japanese subjects (BMI $\geq$ 30 kg/m^2) was 927 (male:female ratio 419:508, age 48.7 $\pm$ 14.2 years, BMI 34.2 $\pm$ 5.4 kg/m^2), whereas that for Japanese normal weight controls (BMI $<$ 25 kg/m^2) was 1,527 (male:female ratio 685:842, age 48.1 $\pm$ 16.5 years, BMI 21.7 $\pm$ 2.1 kg/m^2). The severely obese subjects were recruited from among outpatients of medical institutes. Patients with secondary obesity and obesity-related hereditary disorders were not included, and neither were patients with medication-induced obesity. The normal-weight controls were recruited from among subjects who had undergone a medical examination for screening of common diseases. Clinical features of the subjects are illustrated in Table 1. Additionally, 1,604 subjects were recruited (male:female ratio 803:801, age 48.7 $\pm$ 16.9 years, BMI 22.66 $\pm$ 3.16 kg/m^2) from the Japanese general population. Each subject provided written informed consent, and the protocol was approved by the ethics committee of each institution and that of RIKEN.

DNA preparation and SNP genotyping

Genomic DNA was prepared from the blood sample of each subject by using the Genomix (Talent Srl, Trieste, Italy). We searched for dbSNPs with minor allele frequencies (MAF) $>$ 0.10 in the *FTO* gene of Japanese people. We selected 90 SNPs and were able to construct Invader probes (Third Wave Technologies, Madison, WI)

K. Hamaguchi
Department of Community Health and Gerontological Nursing, Faculty of Medicine, Oita University, Oita, Japan

K. Yamada
Division of Endocrinology and Metabolism, Department of Medicine, Kurume University, Fukuoka, Japan

T. Hanafusa
First Department of Internal Medicine, Osaka Medical College, Osaka, Japan

S. Oikawa
Division of Endocrinology and Metabolism, Department of Medicine, Nippon Medical School, Tokyo, Japan

H. Yoshimatsu · T. Sakata
Department of Anatomy, Biology and Medicine, Faculty of Medicine, Oita University, Oita, Japan

N. Kamatani
Laboratory for Statistical Analysis, SNP Research Center, RIKEN, Tokyo, Japan

Y. Nakamura
Laboratory for Molecular Medicine, Human Genome Center, The Institute of Medical Science, University of Tokyo, Tokyo, Japan

Table 1 Clinical characterization of obese and control subjects

	Obese	Control	*P* value
Gender (M/F)	419/508	658/842	
Age (year)	49.1 ± 14.2	48.2 ± 16.5	0.049
Body mass index (kg/m^2)	34.50 ± 5.39	21.65 ± 2.08	<0.000001
Glucose (mg/dl)	129.2 ± 49.6	97.7 ± 23.9	<0.000001
HbA1c (%)	6.5 ± 1.8	5.1 ± 0.6	<0.000001
Total cholesterol (mg/dl)	209.9 ± 37.9	201.2 ± 36.4	<0.000001
Triglycerides (mg/dl)	153.2 ± 99.5	104.0 ± 73.2	<0.000001
High-density lipoprotein cholesterol (mg/dl)	53.1 ± 18.9	65.1 ± 15.7	<0.000001
Systolic blood pressure (mmHg)	136.4 ± 18.1	123.4 ± 17.8	<0.000001
Diastolic blood pressure (mmHg)	83.8 ± 12.0	76.0 ± 11.1	<0.000001

P values were analyzed using Mann–Whitney *U* test. Data are mean ± standard deviation

for them (Supplementary Table 1). SNPs were genotyped using Invader assays as described previously (Ohnishi et al. 2001; Takei et al. 2002). Nine SNPs (rs9937053, rs9939973, rs9940128, rs7193144, rs8043757, rs9923233, rs9926289, rs9939609, and rs9930506) reported in a previous genome-wide association study (Scuteri et al. 2007) were genotyped using TaqMan probes (C__29910458_10, C__11776771_10, C__29621384_10, C__29387650_10, C__29387665_10, C__29693738_10, C__30270568_10, C__30090620_10, and C__29819994_10; Applied Biosystems, Foster City, CA, USA).

Statistical analysis

Genotype or allele frequencies were compared between cases and controls in three different modes. In the first mode, i.e., the additive mode, χ^2 test was performed according to Sladek et al. (Sladek et al. 2007). In the second mode, i.e., the minor allele recessive mode, frequencies of the homozygous genotype for the minor allele were compared using a 2 × 2 contingency table. In the third mode, i.e., the minor allele dominant mode, frequencies of the homozygous genotype for the major allele were compared using a 2 × 2 contingency table. A test of independence was performed using Pearson's χ^2 method. *P* values were corrected by Bonferroni adjustment and $P < 0.00017$ [0.05/99 (total SNP number)/3 (number of modes)] was considered significant. The odds ratio (OR) and 95% confidence interval (CI) were calculated by Woolf's method. We coded genotypes as 0, 1, and 2, depending on the number of copies of the risk alleles. OR adjusted for age and gender was calculated using multiple logistic regression with genotypes, age, and gender as independent variables. Hardy–Weinberg equilibrium was assessed using the χ^2 test (Nielsen et al. 1998). Haplotype blocks were determined using Haploview (Barrett et al. 2005). Simple comparison of the clinical data among the different genotypes was performed using one-way analysis of variance (ANOVA). Simple comparison of the clinical data between case and control groups was analyzed using Mann–Whitney *U* test. Difference in BMI between genotypes was analyzed using a multiple linear regression, with BMI as the dependent variable and genotype as the independent variable, and with gender and age as covariates for BMI. Statistical analyses were performed using StatView 5.0 (SAS Institute, Cary, NC, USA). Power was calculated by the Monte Carlo method.

Results

Case-control association studies

We searched for dbSNPs with MAF > 0.10 in the *FTO* gene. By using Invader and TaqMan assay, we successfully genotyped 99 SNPs spanning the *FTO* gene (Supplementary Table 1). Using these SNPs, we performed tests of independence between the phenotype and genotypes of obesity at each SNP by using severely obese subjects (BMI ≥ 30 kg/m^2) and normal weight controls (BMI < 25 kg/m^2). For each SNP, the lowest *P* value among the three different modes was selected as the minimum *P* value. All SNPs, including rs1421084, were in Hardy–Weinberg equilibrium ($P > 0.01$) (Supplementary Table 1).

The power of the test was calculated by Monte Carlo method with different MAFs and different effect sizes. Effect of the risk allele on penetrance was assumed to be multiplicative; i.e., the penetrances for three genotypes were assumed to be a, ar, and ar^2, respectively, where a and r denote the lowest penetrance and genotype relative risk, respectively. Supplementary Table 2 shows the calculated values of the power of the test with different MAFs and different genotype relative risks (r). The lowest penetrance (a) was calculated for each gender by assuming the affection rates of 2.3% for men and 3.4% for women (Yoshiike et al. 2002). Genotype relative risk (r) was assumed to be

the same for both genders. Supplementary Table 2 shows that the test has significant power at relative high risk allele frequency when genotype relative risk is >1.7.

As shown in Fig. 1 and Supplementary Table 1, 15 SNPs demonstrated significant associations with the obesity phenotype; the threshold of significance using Bonfferoni correction was $P < 0.00017$. These SNPs included rs9939609 (Frayling et al. 2007) and rs1121980 (Hinney et al. 2007) that were reported to be significantly associated with the obesity phenotype in the Caucasian population, as determined by genome-wide association studies; rs9930506 (Scuteri et al. 2007) showed marginal association with obesity in the Japanese. Linkage disequilibrium (LD) analysis revealed that these 15 SNPs were in almost complete LD ($D' > 0.98$, $r^2 > 0.80$) and were located within the same LD block of approximately 50 kb (Fig. 1). The most significant association was observed for rs1558902 [additive mode, $P = 0.0000041$ and allele-specific OR (95% CI) adjusted for age and gender was 1.41 (1.22–1.62)]. The minor alleles of rs9939609 (MAF = 0.24) and rs1121980 (MAF = 0.26) were significantly more frequent in the obese group than in the normal-weight control group (additive mode, $P = 0.000012$ and $P = 0.000051$, respectively), and ORs were 1.38 (95% CI = 1.20–1.59) and 1.33 (95% CI = 1.16–1.52), respectively (Table 2, Supplementary Table 1). The MAF of both SNPs in the control group was 0.18; this was consistent with data obtained from the haplotype map of the human genome (HapMap) (Supplementary Table 1). Our data indicated that the SNPs in the *FTO* gene were associated with severe obesity in the Japanese.

Analysis of various quantitative phenotypes with rs1558902

To investigate whether the genotypes of SNP rs1558902 are associated with the phenotypes of metabolic disorders, we compared the following among the different genotypes in the cases, controls, and combined groups: ANOVA results, BMI, levels of fasting plasma glucose, hemoglobin A1c (HbA1c), total cholesterol, triglycerides, HDL cholesterol, and blood pressure. As rs1558902 showed the most significant association with obesity and its call rate was the highest, we analyzed various quantitative phenotypes by using this SNP. The quantitative phenotypes regarding BMI and the levels of fasting plasma glucose, HbA1c, total cholesterol, triglycerides, HDL cholesterol, and blood pressure were not found to be significantly associated with the genotypes at rs1558902 in either the case or control group (Table 3). Although there was no significant difference in BMI values among genotypes in either the control or case group, the direction of the difference (AA > AT > TT) was in accordance with the association between the qualitative obesity phenotype and the genotype shown.

Finally, we examined the BMI distribution of rs1558902 in the Japanese general population and found that rs1558902 genotype was significantly associated with BMI

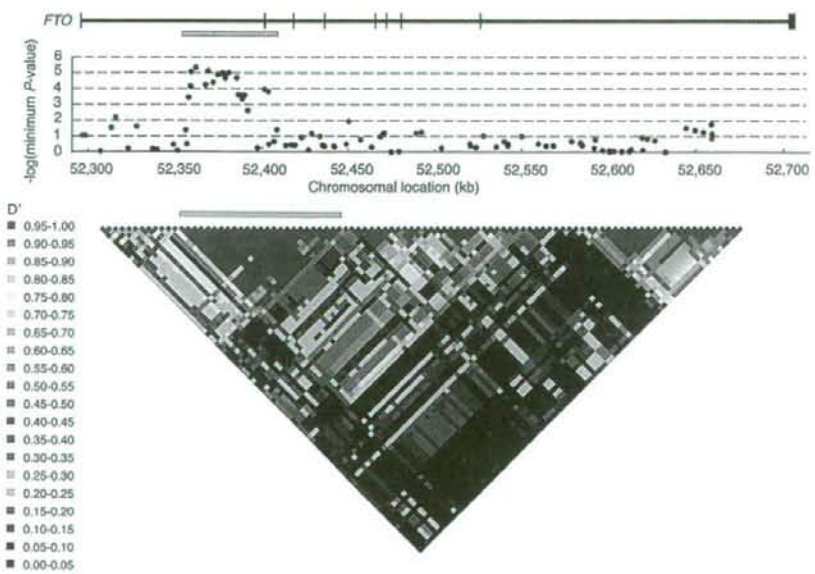

Fig. 1 Linkage disequilibrium (LD) mapping, polymorphisms, and *P* values obtained in the test of independence between the phenotype and genotypes of obesity at various single nucleotide polymorphisms (SNPs) in the fat-mass and obesity-associated gene (*FTO*) gene. *P* values are expressed as negative logarithm of the minimum *P* values obtained in the three models (additive, minor allele dominant, and minor allele recessive modes). LD coefficients (*D'*) between each pair of SNPs were calculated and are displayed as a strand in the LD blocks. Minor allele frequencies of all SNPs used in this analysis are ≥10%. The genomic structure is shown in the *upper*. The *gray bar* marks the LD block associated with obesity

Table 2 Associations of single nucleotide polymorphisms (SNPs) in the fat-mass and obesity-associated gene (*FTO*) gene with obesity existing in the 50-kb linkage disequilibrium (LD) block

dbSNP ID	Allele	Genotype								Additive mode			Recessive mode			Dominant mode		
		Case				Control												
	1/2	11	12	22	Sum	11	12	22	Sum	OR (95% CI)	$\chi 2$	*P* value	$\chi 2$	*P* value	OR (95% CI)	$\chi 2$	*P* value	OR (95% CI)
rs9937053	A/G	59	360	494	913	63	414	773	1250	1.31 (1.13–1.51)	12.3	0.00047	2.0	0.16	1.30 (0.90–1.88)	13.0	0.00031	1.37 (1.16–1.63)
rs9939973	A/G	61	367	496	924	75	504	941	1520	1.32 (1.15–1.51)	15.7	0.000077[a]	3.0	0.081	1.36 (0.96–1.93)	16.1	0.000061[a]	1.40 (1.19–1.66)
rs9940128	A/G	60	366	498	924	75	500	941	1516	1.31 (1.15–1.50)	15.2	0.00010[a]	2.6	0.11	1.33 (0.94–1.89)	15.9	0.000068[a]	1.40 (1.19–1.65)
rs1421085	C/T	49	338	537	924	57	443	1019	1519	1.38 (1.20–1.59)	19.6	0.000011[a]	3.3	0.068	1.44 (0.97–2.12)	20.0	0.0000078[a]	1.47 (1.24–1.74)
rs1558902	A/T	48	341	536	925	52	449	1021	1522	1.41 (1.22 -1.62)	21.2	0.0000041[a]	4.6	0.032	1.55 (1.04–2.31)	20.8	0.0000052[a]	1.48 (1.25–1.75)
rs1121980	A/G	61	367	499	927	73	504	947	1524	1.33 (1.16–1.52)	16.5	0.000051[a]	3.6	0.059	1.40 (0.99–1.99)	16.5	0.000050[a]	1.41 (1.19–1.66)
rs7193144	C/T	49	339	532	920	55	447	1014	1516	1.39 (1.21–1.61)	20.4	0.0000067[a]	4.0	0.044	1.49 (1.01–2.22)	20.3	0.0000067[a]	1.47 (1.24–1.74)
rs8043757	T/A	48	319	541	908	54	436	1027	1517	1.36 (1.18–1.57)	17.4	0.000037[a]	4.2	0.040	1.51 (1.02–2.25)	16.4	0.000052[a]	1.42 (1.20–1.69)
rs8050136	A/C	51	336	538	925	56	450	1018	1524	1.38 (1.20–1.59)	19.4	0.000012[a]	4.7	0.031	1.53 (1.04–2.26)	18.5	0.000017[a]	1.45 (1.22–1.71)
rs3751812	T/G	51	340	534	925	55	458	1013	1526	1.38 (1.20–1.59)	19.6	0.0000098[a]	5.1	0.024	1.56 (1.06–2.31)	18.5	0.000017[a]	1.45 (1.22–1.71)
rs9923233	C/G	51	335	533	919	55	449	1010	1514	1.38 (1.20–1.60)	19.8	0.0000093[a]	5.0	0.025	1.56 (1.06–2.30)	18.7	0.000015[a]	1.45 (1.23–1.72)
rs9926289	A/G	50	323	531	904	56	425	993	1474	1.37 (1.19 -1.58)	18.7	0.000020[a]	3.9	0.047	1.48 (1.00–2.19)	18.1	0.000021[a]	1.45 (1.22–1.72)
rs9939609	A/T	51	334	534	919	56	443	1005	1504	1.38 (1.20–1.59)	19.5	0.000012[a]	4.5	0.034	1.52 (1.03–2.24)	18.7	0.000015[a]	1.45 (1.23–1.72)
rs7185735	G/A	51	340	536	927	55	455	1014	1524	1.38 (1.20–1.59)	19.9	0.0000089[a]	5.0	0.025	1.55 (1.05–2.30)	18.8	0.000014[a]	1.45 (1.23–1.72)
rs9931494	G/C	64	363	494	921	71	504	942	1517	1.35 (1.18–1.55)	18.4	0.000018[a]	5.6	0.018	1.52 (1.07–2.15)	16.9	0.000039[a]	1.42 (1.20–1.67)
rs17817964	T/C	62	361	500	923	68	524	930	1522	1.30 (1.14–1.49)	13.5	0.00022	5.8	0.016	1.54 (1.08–2.19)	11.4	0.00075	1.33 (1.13–1.57)
rs9930506	G/A	67	365	488	920	82	521	913	1516	1.28 (1.12–1.46)	12.8	0.00038	3.5	0.061	1.37 (0.98–1.92)	12.1	0.00051	1.34 (1.14–1.58)
rs9932754	C/T	66	368	491	925	78	525	919	1522	1.29 (1.13–1.48)	13.6	0.00023	4.2	0.040	1.42 (1.01–2.00)	12.6	0.00040	1.35 (1.14–1.59)
rs9922619	T/G	66	368	489	923	78	529	919	1526	1.29 (1.13–1.48)	13.5	0.00024	4.3	0.038	1.43 (1.02–2.01)	12.3	0.00044	1.34 (1.14–1.58)
rs7204609	C/T	134	418	373	925	273	717	529	1519	0.83 (0.73–0.93)	9.68	0.0022	5.0	0.025	0.77 (0.62–0.97)	7.5	0.0063	0.79 (0.67–0.94)
rs12149832	A/G	53	349	525	927	62	480	982	1524	1.33 (1.15–1.53)	15.2	0.000098[a]	3.5	0.061	1.43 (0.98–2.08)	14.8	0.00012[a]	1.39 (1.17–1.64)

The odds ratio (OR) for each SNP was adjusted simultaneously for age and gender using additive model

CI confidence interval, χ^2 chi-square

[a] Significant *P* value ($P < 0.00017$)

Table 3 Comparison of various quantitative phenotypes among different genotypes at single nucleotide polymorphism (SNP) rs1558902 in obese and control subjects

	Obese			Control		
	AA ($n = 48$)	AT ($n = 341$)	TT ($n = 536$)	AA ($n = 52$)	AT ($n = 448$)	TT ($n = 1022$)
Age (year)	49.8 ± 15.3	49.6 ± 14.3	48.8 ± 14.1	46.9 ± 15.4	46.9 ± 16.7	48.8 ± 16.5
P value		0.64			0.098	
BMI (kg/m^2)	35.16 ± 5.70	34.61 ± 5.43	34.39 ± 5.33	21.94 ± 2.23	21.62 ± 2.10	21.65 ± 2.06
P value		0.58			0.56	
Glucose (mg/dl)	142.8 ± 54.8	125.4 ± 43.2	130.8 ± 53.3	101.7 ± 44.1	96.3 ± 18.1	98.2 ± 24.7
P value		0.054			0.34	
HbA1c (%)	6.9 ± 2.1	6.4 ± 1.7	6.5 ± 1.8	5.1 ± 1.2	5.0 ± 0.5	5.1 ± 0.7
P value		0.19			0.15	
Total cholesterol (mg/dl)	215.1 ± 46.7	211.3 ± 38.8	208.6 ± 36.6	195.6 ± 38.8	201.4 ± 37.8	201.4 ± 35.6
P value		0.37			0.53	
Triglycerides (mg/dl)	171.7 ± 119.5	151.3 ± 102.1	153.2 ± 96.0	111.7 ± 70.6	102.0 ± 71.4	104.4 ± 74.2
P value		0.42			0.63	
HDL cholesterol (mg/dl)	53.2 ± 13.8	54.8 ± 24.0	52.0 ± 15.4	62.1 ± 14.2	65.1 ± 15.9	65.3 ± 15.6
P value		0.14			0.53	
SBP (mmHg)	134.2 ± 20.4	137.0 ± 17.8	136.2 ± 18.2	122.7 ± 17.3	123.2 ± 18.8	123.5 ± 17.5
P value		0.61			0.91	
DBP (mmHg)	80.3 ± 11.7	84.1 ± 12.0	83.9 ± 12.0	75.5 ± 11.1	75.2 ± 11.7	76.3 ± 10.9
P value		0.14			0.22	

Data of each quantitative phenotype were compared among different genotypes at the rs1558902 in obese and control subjects. *P* values were analyzed using analysis of variance in each group of obese and control subjects. Data are mean ± standard deviation.

HDL high-density lipoprotein, *SBP* systolic blood pressure, *DBP* diastolic blood pressure.

Table 4 Association of body mass index (BMI) with rs1558902 genotypes in the Japanese general population

	AA	AT	TT	*P* value (additive model)[a]
BMI (kg/m^2) (n)	23.17 ± 3.20 (59)	22.79 ± 3.26 (482)	22.57 ± 3.11 (1063)	0.041

[a] The difference in BMI according to genotypes was analyzed using a multiple linear regression, with BMI as the dependent variable and genotype as the independent variable and with gender and age as covariates for BMI. Data are represented as mean ± standard deviation

(Table 4). This result would confirm the association of rs1558902 with obesity.

Discussion

Recent genome-wide association studies have shown that the *FTO* gene is associated with obesity (Frayling et al. 2007; Scuteri et al. 2007; Hinney et al. 2007). The associations between variations in the *FTO* gene and the obesity phenotype have been observed in many Caucasian subjects (Frayling et al. 2007; Scuteri et al. 2007; Dina et al. 2007; Field et al. 2007; Andreasen et al. 2008; Wåhlén et al. 2008; Peeters et al. 2008). However, these associations were controversial with regard to Asian subjects (Horikoshi et al. 2007; Li et al. 2008; Omori et al. 2008). BMI values did not significantly differ among the genotypes in the general population of Chinese and Japanese (Horikoshi et al. 2007; Li et al. 2008). We performed a case-control association study with regard to severe obesity and found that the SNPs in the *FTO* gene were significantly associated with severe obesity. Although the SNPs demonstrated the most significant association in the Japanese, which was different from that in Caucasians, the significantly associated SNPs existed in a similar block as that in Caucasians. Therefore, the *FTO* gene could also contribute to the development of severe obesity in the Japanese.

BMI was modestly different among rs1558902 genotypes in the general population in this study; rs9939609 was not significantly associated with BMI in the general population (AA 23.22 ± 3.14 vs AT 22.79 ± 3.25 vs TT 22.58 ± 3.13, $P = 0.063$). In the Japanese population, rs1558902 may be more tightly associated with BMI than rs9939609. The National Nutrition Survey of Japan reported that the prevalence of subjects with a BMI of